Oxford Open Materials Science, 2024, **4(1)**, itae004
https://doi.org/10.1093/oxfmat/itae004
Advance Access Publication Date: 25 April 2024
Research article

Application of machine learning and grey Taguchi technique for the development and optimization of a natural fiber hybrid reinforced polymer composite for aircraft body manufacture

Moses Olabhele Esangbedo [1], Bassey Okon Samuel [2,3,*]

[1]School of Management Engineering, Xuzhou University of Technology, Xuzhou, 221018, China
[2]Materials Research Laboratory—Steelagon Engineering Limited, (MRL-SEL), Zaria, Kaduna State 810107, Nigeria
[3]Department of Mechanical Engineering, Faculty of Engineering, Ahmadu Bello University, Zaria, Nigeria

*Correspondence address. Materials Research Laboratory—Steelagon Engineering Limited, (MRL-SEL), 7, Imamu road, Samaru, Zaria, Kaduna State 810107, Nigeria. E-mail: basseyokon59@gmail.com

Abstract

The rapid expansion of the air transport industry raises significant sustainability concerns due to its substantial carbon emissions and contribution to global climate change. These emissions are closely linked to fuel consumption, which in turn is influenced by the weight of materials used in aircraft systems. This study extensively applied machine learning tools for the optimization of natural fiber-reinforced composite material production parameters for aircraft body application. The Taguchi optimization technique was used to study the effect of sisal fibers, glass fibers, fiber length, and NaOH treatment concentration on the performance of the materials. Multi-objective optimization methods like the grey relational analysis and genetic algorithm (using the MATLAB programming interface) were employed to obtain the best combination of the studied factors for low fuel consumption (low carbon emission) and high-reliability structural applications of aircraft. The models developed from regressional analysis had high accuracy of prediction, with R-Square values all >80%. Optimization of the grey relational analysis of the developed composite using the genetic algorithm showed the best process parameter to achieve low weight material for aircraft application to be 40% sisal, 5% glass fiber at 35 mm fiber length, and 5% NaOH concentration with grey relational analysis at the highest possible level, which is unity.

Keywords: machine learning; materials; aircraft structures; optimization; Taguchi; natural fibers; Grey system theory

Introduction

Sustainable transportation refers to low- and zero-emission, energy-efficient, affordable modes of transport, including electric and alternative-fuel vehicles as well as domestic fuels. Generally, sustainable transportation has many advantages, such as energy savings (in the form of fuel costs), cleaner air by the reduction of fossil fuel burning, improved system manufacture and therefore job creation, energy security, and sustainability of material supplies. According to [1], fossil energy and the need for alternative sources remain one of the biggest causes of technological change, and the [2] has noted that transportation as a system is largely dependent on fossil fuels as an energy source. Even though road transport has the highest carbon emissions, the aviation sector is the fastest growing, accounting for 915 million tons of CO_2 in 2019. The industry accounts for about 2.1% of the total global carbon emissions, implying that the emissions from the industry would have put it between Japan and Germany if it were considered an entity in the ranking of countries by emissions [3–6]. Concerning the general transport industry, the aviation industry is responsible for about 35% of total carbon emissions [7]. In the work of [8], it was estimated that the carbon emission tonnage of China between the year 2026–9 will be up to 11.7–127 billion. Reporting data from United Airlines expenses, [9] showed that the expenses of the airline company on fuel alone was up to a 23% of the $38.9 Billion total expense. Such huge fuel consumption is certainly proportional to a vast amount of carbon emission. Such emissions are a result of CO_2 being a major component of the exhaust gas as a result of the burning of aviation fuel during operations, and the operations of the industry are not expected to decline but rather increase since there are currently no significant alternatives or preferred advancements in the transport industry. The structural and policy framework for achieving net zero CO_2 emissions by the year 2050 is captured in the International Energy Agency's (IEA) net zero scenarios, which also align with the main aim of limiting the rise of global temperature by 1.5°C [10–13]. An attempt to reduce CO_2 emissions in the aviation industry will also be a significant step in the achievement of the 2050 net zero goal [14, 15]. CO_2 reduction, apart form cost and reliability has been the major focus of emerging technologies in the aviation industry. Various studies have directly linked the weight of an aircraft to its fuel consumption and proportionally, its emission [16–18].

Emerging technology, a popular concept in the aviation industry, refers largely to the unharnessed innovations. Even though

Received: December 29, 2023. **Revised:** March 11, 2024. **Accepted:** March 23, 2024

much of it has been in regards to efficiency based systems like cleaner fuels, battery powered systems, etc, recent advancements in material science find their best application in aerospace systems [19]. Much advancement in materials science has been a result of solving problems encountered in the aerospace industry [20]. Since the beginning of self-propelled aircraft, the frames of systems have always needed improvement, particularly in terms of weight. These systems are supposed to be developed using lightweight materials that are also reliable and affordable in highly controlled design, development, and manufacturing processes [21]. Even though recent concerns like the sustainability of processes, emissions of engines, etc have been increasingly popular in the aviation industry, the reliability and efficiency of airframes and structures remain at the center stage [22, 23]. Therefore, disruptive technologies like the transition from metal based materials to polymer composites in the development of reliable structures have steadily increased in the aviation industry [24]. Since the positive correlation between the weight of aircraft and fuel consumption has been established, the development of light weighted material will also be a significant contribution to the reduction of fuel consumption, therefore not only reducing the cost of operations of the industry but also reducing the amount of the industry's carbon emissions [25–27].

Polymers are materials that have properties that are incomparable to those of other types of materials like ceramics, steel, wood, etc. With a comparably low density, they are generally cost-effective, corrosion-resistant, and ductile (except for thermosets) [28, 29]. Also, with the transparency and toughness of some of these polymers, they are used as windows and canopies for aircraft instead of glass, which is very brittle [30–32]. But due to their generally low mechanical properties like creep, stiffness, tensile strength, flexural strength, glass transition temperature, etc, they are rarely applied directly without reinforcement. The production of these polymeric materials involves relatively low energy (carbon emissions) when compared to the production of other applicable materials like aluminum and steel [33–36].

Natural fibers are increasingly used by the polymer industry in developing biocomposite materials for wide-ranging applications in the aviation, automotive, agricultural, military, etc industries. Their low cost, availability, and renewability have been their major advantages, mostly due to global economic and political policies concerning process efficiency and environmental preservation [37]. Environmental concerns have been the major drive for emerging technologies for natural fibers, due to their biodegradable characteristics. The environmental friendliness is beyond the biodegradability of the materials also due to the low energy required for their production [38, 39]. Therefore, natural fibers have a critical role to play in transitions from non-renewable resource-based materials to sustainable and greener resource-based materials [40–42]. The growth in the use of fiber-reinforced polymer materials has been due to their distinct properties, such as their strength-to-weight ratio, which has made them a popular topic of discussion both in the industry of material production and in academia. Moreso, there has been growth in the demand for natural fiber-reinforced composites, particularly in the automotive and aerospace industries [43–46]. Liu *et al.* [5] attempted to improve the fracture toughness and the electrical performance of laminates developed from carbon fiber/epoxy composites. The studied nickel-coated carbon fiber (NiCF) veil successfully improved the mode I and mode II fracture toughness by 74.75% and 36.22% respectively. Also, the developed composites still maintained their excellent potential even after delamination. Kastratovi *et al.* [47] studied the mechanical properties of advanced laminate composite materials with a view to aircraft application. The experimental and numerical processes were applied to the study. FE models for predicting failure were developed and the good agreement between simulated and experimental values implies the potential of the model for further improvement. Results have proven natural fiber-reinforced polymer materials to compete favorably with synthetic fibers (glass fibers, carbon fibers, etc) in terms of their mechanical, thermal, and acoustic properties [48]. Their renewability, biodegradability, and recyclability position them as the best for sustainable development and the circular economy. Even with these properties, there is competition between the popularity of metals and composites in the aviation industry. These are a result of the existing technologies, resources, and knowledge base. Billions have been invested in the development of composite materials technologies for aircraft applications, particularly to replace metals like aluminum due to the positive results of reduced fuel consumption, safety, cabin component performance, comfort, etc [49, 50]. One of the aircraft that has significantly applied composite materials to its structures beyond the aircraft boundaries is Boeing's Dreamliner 787 [51]. Since the 1990s, the application of fiber-reinforced composite materials has increased, with the Boeing 787 Dreamliner and the Airbus 350 XWB aircraft using the largest amount for their structures. Moreso, the composite materials account for about 53% of the Airbus airframe, which is a 41% increase when compared to the A330 [52]. The exceptional performance of the 787 Dreamliner has been pegged on the application of these emerging materials science technologies, with composite materials making up 50% of the B787's primary airframe, like the wings and fuselage [53]. The airplane skin too has increasingly had materials studied for its application, and the knowledge of applicable low-cost and sustainable materials for such an application is still limited [54–57]. Hybrid composites, resulting from the amalgamation of different types of fibers, matrices, or reinforcements, offer a versatile platform for achieving a wide range of desired mechanical, thermal, and functional properties. The rationale behind hybrid composites lies in the synergy achieved by combining materials with complementary attributes. For instance, the high strength and stiffness of one type of fiber can be coupled with the impact resistance or toughness of another, resulting in a composite with superior mechanical performance. Additionally, hybridization allows for the optimization of cost-effectiveness, weight reduction, and environmental sustainability by strategically utilizing available resources and minimizing material wastage. Despite the promising potential of hybrid composites, several challenges remain to be addressed, including the optimization of processing parameters, interface compatibility between different components, and the development of reliable predictive models for material behavior [58, 59]. Chemical treatment of fibers is a crucial step in the fabrication of fiber composites, serving several essential purposes to enhance their mechanical properties, processability, and durability. The need for chemical treatment arises from the inherent characteristics of natural fibers, such as cellulose-based materials like sisal, jute, or bamboo, which typically exhibit hydrophilic behavior and lack compatibility with hydrophobic polymer matrices like epoxy or polyester. Chemical treatment addresses these challenges by modifying the surface chemistry of fibers to improve their adhesion to the matrix and overall performance in composite materials [60].

The Taguchi method stands out as one of the most popular and reliable methodologies for experimental design. It is applied to optimizing process parameters within the shortest possible

number of runs. It does this by reducing variations before design optimization to hit the mean target value for output parameters. An orthogonal array is a special tool applied in the Taguchi system to study the various process parameters using the fewest possible experimental runs. One of the novel design aspects of Taguchi's contributions is the emphasis on the study and control of product variability, especially in contexts where achievement of a target mean value for some feature is relatively easy and where high-quality hinges on low variability. But a notable disadvantage of the Taguchi design of the experiment method is its inability to carry out multi-objective optimization. This implies that in cases where more than one criterion determines the optimization, the Taguchi method becomes difficult to apply [45]. Also, grey relational analysis, which has its roots in the gray system theory of [61], has increasingly been used to solve multi-objective optimization problems [62, 63]. In cases of unknown or uncertain information, the gray relational analysis (GRA) system has proven to be very effective at solving issues involving complicated relationships among various alternatives or influences. Some applications of this gray relational analysis are in human resources (the hiring of workers), project planning, quality function deployment, etc The GRA develops solutions for the MADM problems through the combination of the entire range of performance attribute (or effect) values being considered for every alternative (objective) into one single value, reducing the problem into a single objective optimization problem. This process of combining attributes is also applied in some other MADM methods, like SAW and TOPSIS [64]. Esangbedo and Abifarin [65] successfully applied the Taguchi-based grey relational method in the optimization of the multi-objective decision problems in which the compromise between quality and cost of the manufacturing process was considered. A high-quality machining process with the optimal combination for the best quality at the lowest cost was derived.

Machine learning (ML) is a statistical method for analyzing and drawing conclusions from data that employs a range of algorithms designed to address various sorts of queries [66, 67]. ML may be classified into three categories: reinforcement learning, unsupervised learning, and both. In supervised learning, ML techniques may be used to simulate relationships between one or more independent variables and a dependent variable. In unsupervised learning, algorithms identify significant trends in datasets or categorize data [68]. When given a set of restrictions or a reward structure, reinforcement learning machine learning algorithms create efficient plans or courses of action [69]. The intricacy of designing with composite materials has made optimization approaches, such as the use of a GA, more and more convenient. The optimization methodology called GA is based on simulating Darwin's theory of evolution [70, 71]. The GA generates an acceptable population from a randomized population using fitness goal-based operators. The benefit of GAs is that they provide the designer with a family of nearly optimum designs instead of only one with a tiny difference in the performance index [72]. Evolution, including the ideas of mutation, natural selection, inheritance, and crossover, served as inspiration for genetic algorithms (GAs). A GA modifies an initial dataset one attribute at a time and "runs" it through hundreds or thousands of "generations" to evaluate the outcome and give each attribute a specified weight [73]. GAs are used to tackle optimization, classification, and prediction issues.

Sustainability entails long-lasting changes that meet current needs without compromising future generations. It goes beyond maintainability, ensuring positive impacts without harming others or the environment. This global focus reflects increasing awareness of human activities' environmental consequences. Even with the increasing conversation on the concept of sustainable technology (sustainability) in transport, much focus has been given to the development of transportation systems (solar powered aircraft, electric cars, etc), but less focus has been given to the sustainability of the materials used for developing these technologies. Gossling and Lyle [74] studied the sustainability of the aviation industry based on transition policies and noted that a reduction in aviation emissions is possible but will require policies at various levels. This highlights the importance of local efforts to reduce carbon emissions rather than relying on mainstream policy. Buendia-Hernandez *et al.* [75] applied the two-variable system to model the emissions of air traffic. In the study, the relationship between the number of users of air transport and the emissions in the industry was established. With feedback in terms of technological innovations and socioeconomic responses, it was discovered that emission stabilization was unsuccessful, although the growth rate was slowed. Huang *et al.* [76] studied the correlation between lightweight aircraft and emissions. In the study, additive manufacturing was established as a viable method for the improvement of material performance with respect to weight reduction and the reduction of greenhouse gas emissions. Al-Fatlawi *et al.* [77], in their production of a polymer-based natural fiber-reinforced lightweight polymer for aircraft structural applications, succeeded in the optimization of the material and reported a weight savings of 66% when compared to the application of aluminum. In their study, it was noted that weight reductions result in a reduction of fuel consumption and, therefore, a simultaneous reduction in emissions or damage to the environment. Setlak *et al.* [78] characterized comparatively modern materials used for the development of aircraft structures, with much focus on the airframe. It was noted that the application of computational methods in the modeling and design of aircraft structures was significant in facilitating the procedure. It was also noted that a reduction in the weight of the aircraft through the development of advanced materials for such functions would not only reduce carbon emissions but also have the potential to reduce the cost of manufacturing. Shrivastava *et al.* [79] used the CAE solver based on the genetic algorithm method to optimize the weight of multi-laminate materials for application in aircraft structures. The study aimed to minimize the weight of the material while maximizing its strength and stiffness. Reducing multiple fitness functions to one function was a multi-objective optimization problem that resulted in the reduction of the weight of the aircraft wing torsion box by 29% when compared to similar material and a reduction of weight by 54% when compared to aircraft models designed with metals. Seeger and Wolf [80] applied a design concept database method for combining multi-objective optimization with parameterized simulation modeling for the optimization of aircraft parts (fuselage) that are developed with composite material. The method developed, although targeted for the study of very complex aircraft parts, can be used for the optimization of various aircraft structures. Morse *et al.* [81] studied the application of the genetic algorithm and deep neural network to the optimization of the manufacturing cost of aircraft structural parts developed from composite materials. Even though the process cost was the main target, reliability was a strong influence on the optimization, and the result of the study proved the significance of various manufacturing parameters on the reliability-based cost of the composite materials developed for aircraft structures. Das *et al.* [82] extensively reviewed the application of artificial intelligence

techniques in the prediction of the failure of aircraft structures and the advantages of these advanced computational techniques on the development of materials, and performance monitoring was noted. Alhajahmad and Mittelstedt [83] attempted to optimize the design of a stiffened fuselage skin for aircraft structures. Modeling of the problem was carried out using a Python abacus, and optimization using a genetic algorithm was effected in the MATLAB environment. The study revealed the possibility of reducing the weight of the aircraft structure by 30% and 18% for the different types of grids considered. Even though other synthetic fiber reinforced composites has proven to show more mechanical reliability and structural strength than natural fiber reinforced composites, they are still susceptible to environmental degradation. This was proven in the work of [84] in which the tensile strength of carbon fiber reinforced polymer composites with different angle of fiber alignment was tested as different hygrothermal conditions. The result of the study showed that the even with its initial good mechanical properties, exposure to these conditions were adversarial to the material in terms of its mechanical performance. Ricci *et al.* [85] optimized the weight of the LASER aircraft structure using a multi-objective optimization strategy. With a focus on the wing structure of the mentioned aircraft, the work optimized the internal material design for the aircraft part. Major findings of the study showed that carbon fiber with an angular orientation of 0° on the main spar flange and 25% on the chord produced the best performance for the development of materials for winged structures. Ali and Haron [86] noted the low factor of safety applied in the design of aircraft wings due to the low weight expected and thus applied the ANSYS software tool in the optimization of laminated composite materials design for excellent performance in terms of weight, stiffness, and strength. The results showed the application of symmetric cross-ply laminates will result in higher performance for the design of aircraft wings. Sarangkum *et al.* [87] proposed methods for the optimization of designs of aircraft fuselages for better performance in terms of their weight, compliance, and first-mode natural frequency. To achieve this, multiple multi-objective optimization methods, which are heuristic, were applied and their different results were compared. The result of the study was increased structural efficiency of the aircraft fuselage as per the design. To the best of our knowledge, this is the first study that reduces carbon emission by optimizing the materials for low-fuel aircraft manufacture using the genetic algorithm approach on natural fibers hybridized with synthetic fibers.

This present study

This study presents an extensive study into the possibility of developing materials for aircraft body applications from natural fibers to achieve weight reduction and therefore reduction in carbon emissions without compromising performance. It seeks the optimal quantity in which synthetic fibers (glass fibers) can be replaced by natural fibers in the development of aircraft structures. Different optimization techniques are applied, but significantly, the machine learning method (the genetic algorithm) is applied to models obtained from single objective optimization (Taguchi) and multi-objective optimization (grey relational analysis) to determine these optimal combinations of the material manufacturing process parameters. The main contribution of this study is the development of lightweight materials for low fuel consumption in the aviation industry.

Experimental methods

Figure 1 gives a diagrammatic representation of the study procedure. It shows the procedure for material development and the methods employed for optimization.

Figure 6A–D present the effects of the various factors on the density of the developed composite. It shows how much these factors affect the fuel consumption of aircraft developed with composite materials. It is observed that increasing the sisal fiber and glass fiber loading also increases the density of the material. These imply that both the sisal and the glass fibers will have a negative influence on aircraft fuel consumption. It was also observed that increasing the fiber length of the material increases its density as well. A notable observation is that increasing the concentration of NaOH reduced the density of the material. This is not disconnected from the removal of the dense matter (lignin) from the density of the material.

Fiber treatment

The sisal fiber obtained was extracted from locally sourced sisal leaves using the method of [88]. Before alkalization (treatment), the extracted fibers were washed thoroughly using distilled water and dried at a temperature of 50°C for 24 h. The dried sisal fibers were then treated by immersing them in an aqueous solution of NaOH at different percentages as in the design of the experiment. The immersed fibers are left in the solution for 3 h at 70°C. The treated fibers are then de-alkalinized (neutralized) in a 5% acetic acid solution. The de-alkalized fibers are then thoroughly washed in plenty of distilled water and oven dried for 12 h at 70°C.

Composite development

The composites were developed by the open mold hand layup method. The treated sisal and glass fibers (which were obtained from Sigma Aldrich chemicals) were cut to length as prescribed by the orthogonal array. The epoxy matrix and the hardeners used were also obtained from Sigma Aldrich Chemical Company (Merck). The epoxy and matrix were mixed in a ratio of 5 : 1, and the cut fibers (sisal and glass) were introduced into the mixture according to the experimental design and mixed thoroughly before being poured into the open steel mold, which had a dimension of 300x300x3 mm. The mold was initially smeared with wax to aid in easy removal. Brushes were used to spread the mix evenly on the mold cavity, and roller brushes were used to remove entrapped air in the composite. The mixtures in the mold were then transferred to the hydraulic press, where they were kept under a pressure of 15 MPa for 72 h. This further helped remove voids in the material. The set materials were then removed from the mold and trimmed. The production process of the composite is detailed in Fig. 1B. Different samples for the different tests were cut out of the developed composites. Figure 2 shows pictorial samples of the developed composite materials.

Mechanical and physical tests

Tensile test

The tensile strength of the developed composites was tested according to ASTM D638-14. The procedure was carried out on the Instron 5567 universal testing machine at a crosshead speed of 1.0 mm/min. The tensile strength was then obtained using Equation (2).

$$Stress = \frac{Force}{Area} \tag{1}$$

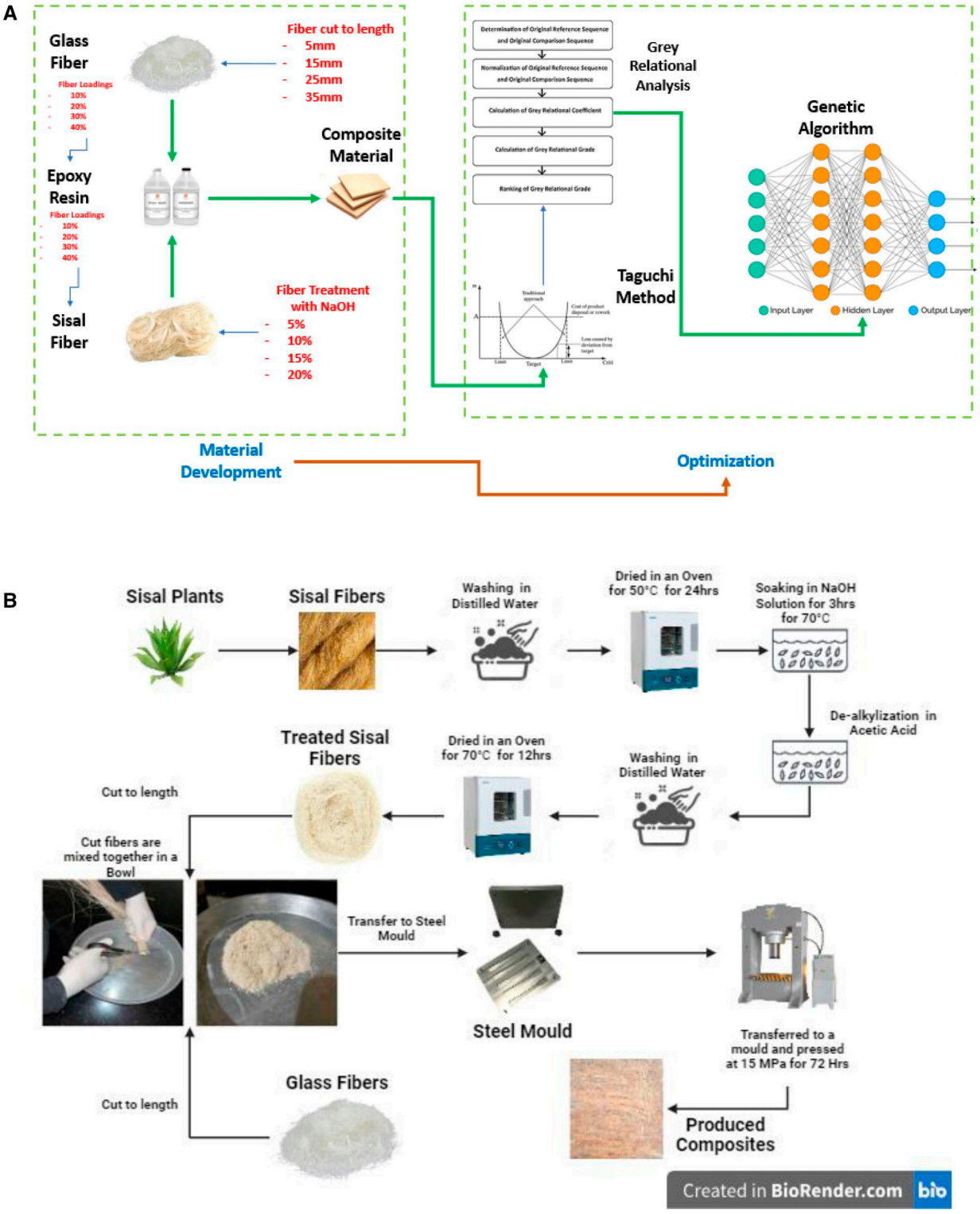

Figure 1. (**A**) Experimental/study procedure. (**B**) Production process of the composite.

$$Tensile\ Strength = \frac{Load\ at\ Break}{(Original\ width)(Original\ thickness)} \quad (2)$$

Flexural test

The universal testing machine Instron 3365, set at a span length of 40 mm and a crosshead speed of 10 mm/min, was used for testing the flexural strength of the material according to ASTM 7264-21. The dimensions of the flexural test samples were 60 mm in length, 10 mm in width, and 3 mm in thickness. The flexural test was carried out on three samples for each combination (run), and the average was recorded. This was for replicability. The flexural strengths were then determined by Equation (3).

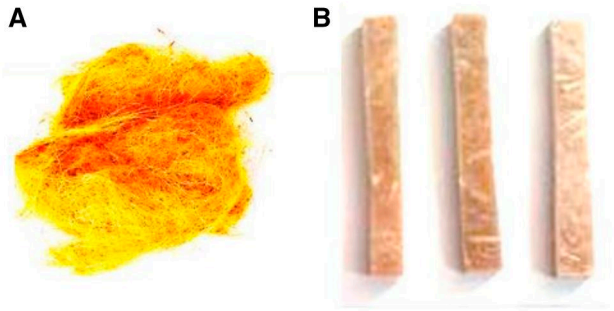

Figure 2. (**A**) Cured sisal fiber. (**B**) Developed composite.

$$Flexural\ Strength = \frac{3PL}{2bt^2} \tag{3}$$

With L being the length of the samples, P is the maximum load applied, and b is the width with t as the thickness of the samples.

Impact test

The impact test was carried out using the PANTECH instrumented pendulum, Model XC-50, set a 1 × 220 V × 60 Hz. The samples for the test were prepared according to the dimensions specified by ASTM D6110-18.

Density

The water displacement method (Archimedes principle) was used to obtain the density of the materials. The volume of the displaced water was used to calculate the density of the material as in Equation (3), where ρ is the density, the mass is defined as m (which was measured directly from the digital weighing balance), and v is the volume of the water displayed.

$$\rho = \frac{m}{v} \tag{4}$$

Optimization

Taguchi and grey's approach to robust parameter design

Taguchi robust design of experiment

In the Taguchi technique of optimization, the optimal combination of various factors to produce the best effect is obtained. It is initiated through the means of lesser variability by the technique of the signal-to-noise ratio, wherein the noise (uncontrolled effects) is greatly reduced to amplify the expected (controlled) effect. This is either by considering the measured effect for the highest measured value (maximum), termed "higher the better," the lowest measured value (minimum), referred to as "lower the better," or a target value (range), referred to as "nominal the best." This implies that an effect such as customer patronage, the quality of airport services, passenger satisfaction, safety, etc is expected to be at the highest possible value and is therefore referred to as "the higher the better." The cases of weight and cost of aircraft maintenance, fuel consumption, time of aircraft maintenance, flight delay, etc are expected to be at their lowest possible value, and therefore they are referred to as "lower the better." The S/N ratios for the higher the better, the lower the better, and nominally the best are obtained using Equations (4–6), respectively.

$$\left(\frac{S}{N}\right)_{HTB} = -10 * log_{10}\left(\frac{1}{n}\sum_{i=1}^{n}\frac{1}{y_i^2}\right) \tag{5}$$

$$\left(\frac{S}{N}\right)_{STB} = -10 * log_{10}\left(\frac{1}{n}\sum_{i=1}^{n}y_i^2\right) \tag{6}$$

$$\left(\frac{S}{N}\right)_{NTB} = 10 * log_{10}\left(\frac{1}{n}\sum_{i=1}^{n}\frac{\bar{y}^2}{S^2}\right) \tag{7}$$

Where n is the number of experiments, y_i represents the response value of the i^{th} an experiment in the orthogonal array, $\bar{y}^2$ indicates the mean, and S^2 the variance of the observed data. Table 1 presents the effects considered as a criterion for the optimization. In this study, the optimization objective is to achieve high tensile, flexural, impact strength, and low density. The factors under study include sisal fiber loading, glass fiber loading, fiber length, and sisal fiber treatment concentration. These factors and the various levels are presented in Table 2. Also, Table 3 presents the orthogonal array on the design of the experiment.

Experiments on the runs (tensile, flexural, impact, and density tests) were performed three times for repeatability, and the obtained values were further processed for modeling and optimization. Optimization of the effects was carried out via the Taguchi method, wherein the tensile, flexural, impact, and density of the material was optimized based on "higher the better" and the density optimized based on "lower the better." It is expected that a decrease in weight will correspond to a decrease in fuel consumption and therefore a decrease in emissions.

The optimum effect via the optimum combination is predicted using Equation (8). Where: T_m is the overall mean of (tensile, flexural, impact strength, and density); T_{ijmax} is the mean effect at optimum level i of factor k and k_n is the number of main design factors that affect the response. T_{ijmax} was obtained from the response table of mean or S/N ratio in which for each parameter on the table, the highest value among the levels is the T_{ijmax}. Analysis of variance is then carried out to observe the significance of the process parameters on the material development for aircraft structures.

$$T_{opt} = T_m + \sum_{k=1}^{k_n}\left[(T_{ik})_{max} - T_m\right] \tag{8}$$

Optimization process confirmation

Confirmation of the predicted effects is carried out by redeveloping the materials in the optimal combination, testing the various effects, and comparing the experimented values with the predicted values based on the confidence interval obtained from Equation (9).

$$C.I = \sqrt{F_\alpha(1, F_e)V_e\left[\frac{1}{\eta_{eff}} + \frac{1}{\eta_{ver}}\right]} \tag{9}$$

Where; C. I = Confidence interval; $F_\alpha(1, F_e) = F$ ratio required for α; α = Risk; F_e = Error DOF; V_e = Error Variance (obtained from the Anova Table); η_{ver} = number of trials to run confirmation test I.e. same as the number of replication for each run; η_{eff} = the Effective number of replications and was calculated using

Table 1. Optimization effects

S. No.	Effect	Criteria
1	Tensile strength	Higher the better
2	Flexural strength	Higher the better
3	Impact strength	Higher the better
4	Density	Lower the better

Table 2. Factors and levels considered for the production of the natural fiber-reinforced composites

Factors		Levels			
		1	2	3	4
Sisal fiber loading (%)	A	10	20	30	40
Glass fiber loading (%)	B	20	15	10	5
Fiber length (mm)	C	5	15	25	35
NaOH conc. (%)	D	5	10	15	20

Table 3. Orthogonal array of the factors under consideration

Runs	Factors combination			
	A	B	C	D
1	10	20	5	5
2	10	15	15	10
3	10	10	25	15
4	10	5	35	20
5	20	20	15	15
6	20	15	5	20
7	20	10	35	5
8	20	5	25	10
9	30	20	25	20
10	30	15	35	15
11	30	10	5	10
12	30	5	15	5
13	40	20	35	10
14	40	15	25	5
15	40	10	15	20
16	40	5	5	15

Equation (10) and the percentage error was obtained from Equation (14). The percentage error is calculated using Equation (11).

$$\eta_{eff} = \frac{N}{1 + [Total\ DOF\ of\ controlled\ factors]} \tag{10}$$

$$Error = \frac{Experimental\ value - Predictive\ Value}{Experimental\ Value} \tag{11}$$

Grey relational analysis

As earlier stated, the drawback of the Taguchi optimization technique is its singularity. In that case, only one effect can be optimized. As in this study, the Taguchi optimization technique can only determine the optimal process parameters for obtaining the best tensile, flexural, or impact strength or the optimal process parameters for the lowest density. In conditions where there is more than one optimization criterion, it becomes impossible to use the Taguchi optimization technique. Such as in the development of materials for lightweight (low fuel consumption) aircraft structures, and where the materials must also be strong, other optimization techniques that are multi-objective must be explored. In such cases, there is the necessity of compromising one effect over another while still keeping performance at its possible maximum. Multi-objective optimization makes it possible to have the optimum point where the weight can be as light as possible while still being at the lowest possible cost. In this study, the tensile, flexural, and impact strengths of the materials are optimized while keeping the density of the material as low as possible. Gray relational analysis is a tool for carrying out such tasks as multi-objective optimization. Samuel *et al.* [89] applied the GRA to the optimization of materials for the development of wind turbine blades. In the GRA method, normalization of the various effects is carried out to reduce the variations in quantities. Equation (12) is used for the normalization process on effects for "the "higher the better" and Equation (13) for normalizing effects for "the lower the better." Where $x_i^*(k)$ is the sequence after the data processing i.e. for the i^{th} experiment and the k^{th}response and $x_i(k)$ is the comparability sequence. In this study, the Tensile, flexural and impact strength will be normalized for "the higher the better" and the density of the material will be normalized for "the lower the better." Thereafter, the deviation sequence (which implies the deviation of the normalized values from a reference sequence is obtained using Equation (14). The reference sequence in this study is taken as 1 for all the responses. That is $x_0^*(k) = 1$ and $\Delta_{0i}(k)$ is the deviation sequence. Then the grey relational coefficient (GRC), $\xi(k)$, is calculated using Equation (15). The GRC is an expression of the relationship between the actual normalized results and the ideal. The grey relational grade γ_i was calculated which is the average of the coefficients from each factor for each run. The grey relational grade γ_i is expressed in Equation (16). Where γ_i= Grey relational grade for i^{th}experiment, n = number of performance characteristics, which is the number of k or the number of responses. The grey relational grades are then ranked and the Taguchi technique is carried out on the GRG for optimization of the control factors.

$$x_i^*(k) = \frac{x_i(k) - minx_i(k)}{maxx_i(k) - minx_i(k)} \tag{12}$$

$$x_i^*(k) = \frac{maxx_i(k) - x_i(k)}{maxx_i(k) - minx_i(k)} \tag{13}$$

$$\Delta_{0i}(k) = \left|x_0^*(k) - x_i^*(k)\right| \tag{14}$$

i.e $\Delta_{0i}(k) = |1 - normalized\ value\ of\ the\ response|$

$$\xi(k) = \frac{\Delta_{min} + \zeta\Delta_{max}}{\Delta_{0i}(k) + \zeta\Delta_{max}} \tag{15}$$

$$\gamma_i = \frac{1}{n}\sum_{k}^{n}\xi_i(k) \tag{16}$$

Machine learning (genetic algorithm)

Machine learning tools like genetic algorithms will be used for the optimization of the effects under study. For this study, the genetic algorithm method was applied as in [90]. Objective functions were derived from regression models of the effect of the combination of the Taguchi runs. The MATLAB 8.0 interface was used for the genetic algorithm optimization. The default parameters for the MATLAB genetic algorithm optimization are employed in this study. A forward migration direction was

applied to a population size of 20 with a rank fitness scaling function. A cross-over probability of 0.8 at a constrained dependent mutation function and scattered cross-over were also employed. The stochastic method was applied to the models of tensile, flexural, impact, and density strengths. Also, the model obtained from the gray relational analysis on the gray relational grade was optimized based on the uniqueness of the optimization method.

Results and discussions

The results of the tensile, flexural, impact and density tests are presented in Table 4, where the average tensile, flexural, impact, and density strengths are observed to be 69.3 MPa, 58.22 MPa, 29.0 kJ/m^2, and 0.8267 g/cm^3, respectively. Also, the average S/N ratio based on "the higher the better" for the tensile, flexural, and impact tests is 36.74 dB, 35.25 dB, and 28.49 dB, respectively. while the general means for the density based on "the lower the better" is 1.7093 dB. Also, Table 5 presents the mean and S/N ratio response means. It is observed that the sisal fiber loading had more significance on the tensile and flexural strengths of the developed material, with a delta of 18.43 and 6.97, respectively. The glass fiber was observed to have a higher effect on the impact strength and density of the material than the sisal fiber loading, with it having the best rank. The effect of these factors (process parameters) on the tensile, flexural, impact and density of the material is shown graphically in Figs 3–6.

Figure 3A shows that the optimum tensile strength is obtained at a sisal fiber loading of 20%, beyond which there is a drop. The initial rise in the tensile strength with increasing fiber loading is due to the good fiber-to-polymer (interfacial) adhesion as a result of the treatment with NaOH. This may be a result of the covalent bond between the fiber surface and the polymer, as reported by [91]. The further drop may be attributed to the increase in fiber ends (therefore, an increase in possible failure initiation points).

Figure 3B, which depicts the effect of glass fiber loading on the tensile strength of the material developed for aerospace applications, shows that the glass fiber had a positive influence on the tensile strength of the material up until 15% fiber loading. Synthetic fibers like glass fibers, carbon fibers, and Kevlar have been established to have higher strength than natural fibers. Figure 3C shows the increase in tensile strength as a result of the increase in fiber length. The increase in tensile strength is due to an increase in the surface area through which effective stress transfer from the matrix to the reinforcement occurs.

The NaOH is observed to have a non-linear effect on the tensile strength of the material. Even though it is observed that there is an increase in the tensile strength of the material with an increase in the NaOH concentration beyond 15% of the alkali, Narayana and Rao [92] also reported an increase in the tensile strength of the material with an increase in the alkali treatment concentration. The observed variation in tensile strength could be attributed to the intricate interplay between NaOH concentration and its effects on fiber-matrix interaction. While a certain level of NaOH treatment enhances the bonding between fibers and the epoxy matrix, excessive treatment may lead to over-processing, causing degradation of the fibers and consequently compromising mechanical properties. The decrease in tensile strength at higher NaOH concentrations could be indicative of this phenomenon, where the aggressive treatment might have resulted in fiber degradation, leading to reduced load-bearing capacity. It's possible that the optimal NaOH concentration lies within a certain range, beyond which diminishing returns or even detrimental effects on mechanical properties are observed.

Figure 4A shows that the flexural strength of the natural fiber composite increased with an increase in the loading of sisal fibers. Natural fibers like sisal and pineapple leaf fibers are known to be advantageous in improving the flexural strength of polymer composites. The maximum flexural strength was thereby observed to be 61.06 MPa at a sisal fiber loading of 40%.

The optimum flexural strength of 63.52 MPa was obtained at a glass fiber loading of 15%, as observed in Fig. 4B. Even though it was observed that the flexural strength of the composite generally increased with an increase in the loading percentage of the glass fiber, beyond 50%, a decline in the glass fiber was observed. This decline in the glass fiber may be due to the effect of fiber-to-fiber interaction. This observation agrees with the report of [93], where the increase in fibers beyond a particular level resulted in the reduction of flexural strength by up to 9%.

Table 4. Mean and S/N ratio of tensile, flexural, impact, and density of the developed composite

S/N	Factors				Effects							
	A	B	C	D	Tensile strength		Flexural strength		Impact strength		Density	
					Mean (MPa)	S/N (dB)	Mean (MPa)	S/N (dB)	Mean (kJ/m^2)	S/N (dB)	Mean (g/cm^3)	S/N (dB)
1	10	20	5	5	48.4	33.70	44.7	33.00	7.3	17.32	0.6113	4.2745
2	10	15	15	10	58.1	35.28	52.2	34.36	19.8	25.92	0.7383	2.6349
3	10	10	25	15	62.6	35.93	60.5	35.64	25.5	28.13	0.7936	2.0080
4	10	5	35	20	60.4	35.63	59	35.42	23.6	27.45	0.7920	2.0253
5	20	20	15	15	66.1	36.40	49.5	33.90	10.2	20.17	0.6916	3.2034
6	20	15	5	20	73.1	37.28	57.2	35.15	27.0	28.62	0.8274	1.6458
7	20	10	35	5	83.4	38.43	65.7	36.34	40.7	32.19	0.9323	0.6094
8	20	5	25	10	80.6	38.12	60.9	35.69	35.8	31.07	0.8974	0.9398
9	30	20	25	20	70.8	37.00	52.3	34.36	28.5	29.08	0.7628	2.3524
10	30	15	35	15	74.7	37.47	61.6	35.79	37.4	31.46	0.9023	0.8929
11	30	10	5	10	74.8	37.48	62.1	35.86	31.7	30.02	0.8413	1.5011
12	30	5	15	5	75.1	37.51	61.5	35.78	37.5	31.48	0.8859	1.0521
13	40	20	35	10	65.1	36.27	53.7	34.59	27.0	28.62	0.8046	1.8888
14	40	15	25	5	71.5	37.09	63.1	35.99	39.7	31.98	0.9311	0.6199
15	40	10	15	20	73.1	37.28	65.8	36.37	40.2	32.08	0.9377	0.5590
16	40	5	5	15	70.5	36.96	61.7	35.81	32.7	30.29	0.8769	1.1412
				Average	69.3	36.74	58.22	35.25	29.0	28.49	0.8267	1.7093

Table 5. Response table for means

Levels	Tensile strength							
	Sisal fiber loading (%)		Glass fiber loading (%)		Fiber length (mm)		NaOH conc. (%)	
	Mean (MPa)	S/N ratio (dB)	Mean (MPa)	S/N ratio (dB)	Mean (MPa)	S/N ratio (dB)	Mean (MPa)	S/N ratio (dB)
1	57.37	35.13	71.63	37.05	66.69	36.35	69.61	36.68
2	75.8	37.56	73.47	37.28	68.08	36.62	69.63	36.79
3	73.84	37.36	69.35	36.78	71.36	37.03	68.45	36.69
4	70.04	36.9	62.6	35.84	70.91	36.95	69.35	36.8
Delta	18.43	2.43	10.87	1.43	4.67	0.68	1.17	0.11
Rank	1	1	2	2	3	3	4	4
	Flexural strength							
	Mean (MPa)	S/N ratio (dB)	Mean (MPa)	S/N ratio (dB)	Mean (MPa)	S/N ratio (dB)	Mean (MPa)	S/N ratio (dB)
1	54.09	34.6	60.78	35.67	56.41	34.95	58.71	35.28
2	58.33	35.27	63.52	36.05	57.28	35.1	57.21	35.13
3	59.35	35.45	58.51	35.32	59.18	35.42	58.33	35.28
4	61.06	35.69	50.02	33.96	59.97	35.54	58.57	35.32
Delta	6.97	1.09	13.5	2.09	3.56	0.58	1.5	0.2
Rank	2	2	1	1	3	3	4	4
	Impact strength							
	Mean (kJ/m^2)	S/N ratio (dB)	Mean (kJ/m^2)	S/N ratio (dB)	Mean (kJ/m^2)	S/N ratio (dB)	Mean (kJ/m^2)	S/N ratio (dB)
1	19.04	24.7	32.39	30.07	24.67	26.56	31.33	28.25
2	28.41	28.01	34.52	30.61	26.91	27.41	28.55	28.91
3	33.77	30.51	30.97	29.49	32.36	30.07	26.45	27.51
4	34.89	30.74	18.24	23.8	32.16	29.93	29.79	29.31
Delta	15.85	6.04	16.28	6.81	7.69	3.51	4.88	1.8
Rank	2	2	1	1	3	3	4	4
	Density							
	Mean (g/cm^3)	S/N ratio (dB)	Mean (g/cm^3)	S/N ratio (dB)	Mean (g/cm^3)	S/N ratio (dB)	Mean (g/cm^3)	S/N ratio (dB)
1	0.7338	2.736	0.8631	1.29	0.7892	2.141	0.8402	1.639
2	0.8372	1.6	0.8762	1.169	0.8134	1.862	0.8204	1.741
3	0.8481	1.45	0.8498	1.448	0.8462	1.48	0.8161	1.811
4	0.8876	1.052	0.7175	2.93	0.8578	1.354	0.83	1.646
Delta	0.1537	1.683	0.1587	1.76	0.0686	0.787	0.0241	0.172
Rank	2	2	1	1	3	3	4	4

The effect of the fiber length on the flexural strength of the materials is shown graphically in Fig. 4C, where it is observed that the increase in the flexural strength of the material with the increase in fiber length was almost linear. This is not disconnected with the ease of stress transfer from the matrix to the fibers due to increased surface area. The peak flexural strength obtained at 35 mm fiber length was 59.97 MPa.

Figure 4D, which depicts the effect of NaOH on the flexural strength of the developed composite, shows an initial drop in the flexural strength with an increase in the concentration of NaOH from 5% to 10%. This decrease may be due to insufficient degumming (lignin removal) from the surface of the fibers. This causes reduced interfacial bonding between the matrix and the fibers. The reverse effect on the flexural strength beyond 10%, leading to an increase, is a result of the proper treatment of the surface. At these higher concentrations, total lignin removal is achieved, as is an even further roughening of the surface for proper bonding of the matrix.

From Fig. 5A, the peak impact strength of the developed composite, which had a sisal fiber load of 40%, is 34.89 kJ/m^2. Even though the impact strength increased with a corresponding increase in the sisal fiber loading, beyond 30%, the rate of increase was reduced. This may be due to the formation of voids at higher loadings, leading to an increase in possible crack initiation and propagation sites.

In Fig. 5B, increasing the glass fiber loadings has a corresponding increase in the impact strength of the material. The peak impact strength is 34.52 kJ/m^2 at a glass fiber content of 15%. This increase in the impact strength of the fiber is due to the high impact strength of the glass fiber and the good interfacial adhesion of the glass fibers to the matrix material.

In Fig. 5C, it is observed that the fiber length of the reinforcement proportionally increases the impact strength of the material. This is still tied to the large surface areas over which the impact energy can be easily transferred to the reinforcement. Moreso, the longer the fibers are, the fewer ends there are through which cracks can easily propagate.

In Fig. 5D, the effect of NaOH on the impact strength of the developed composite is presented. It shows that below 15% NaOH concentration for the treatment of the fiber, there is a reduction in impact strength with an increase in the NaOH concentration. Beyond 15%, the influence of NaOH on the impact strength of the material is positive. The best impact strength obtained for this factor is 31.33 kJ/m^2.

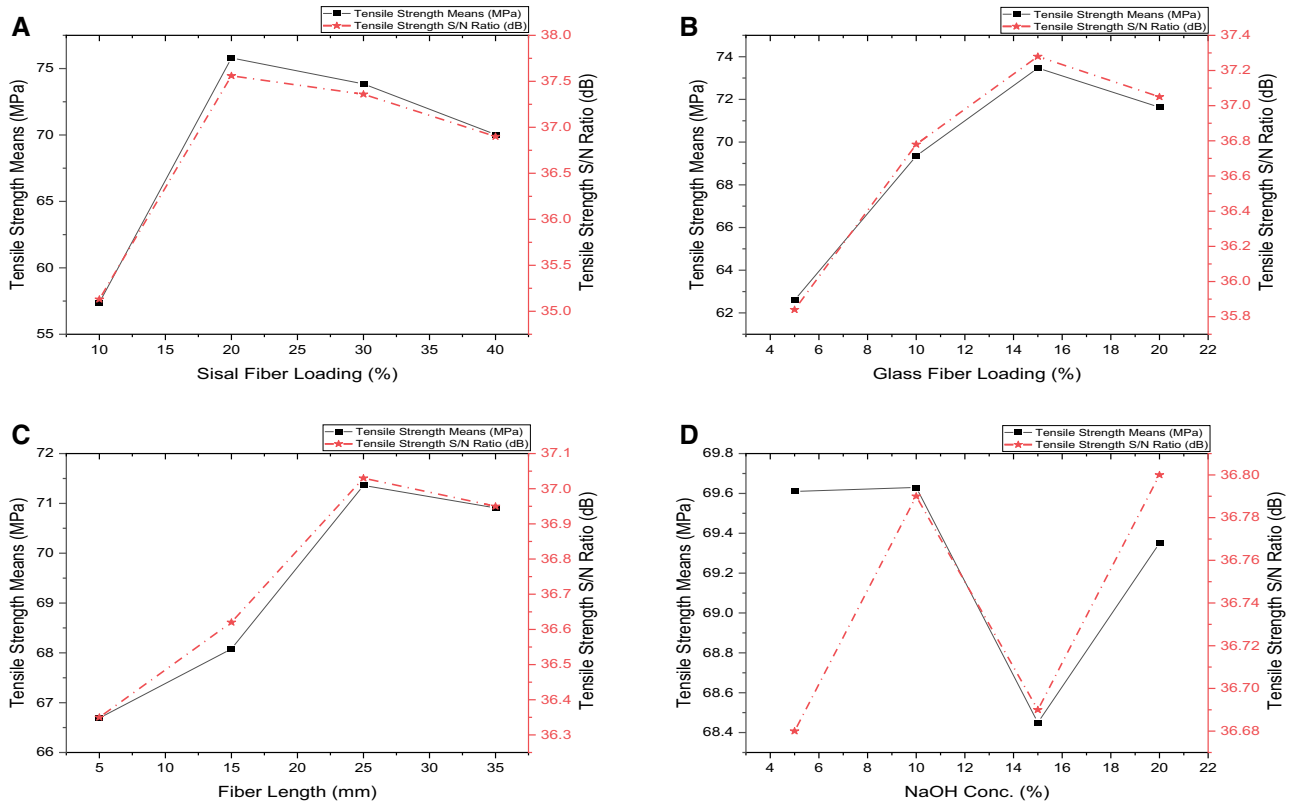

Figure 3. (**A**) Effect of sisal fiber loading on the tensile strength of the developed composite. (**B**) Effect of glass fiber loading on the tensile strength of the developed composite. (**C**) Effect of fiber length on the tensile strength of the developed composite. (**D**) Effect of fiber length on the tensile strength of the developed composite.

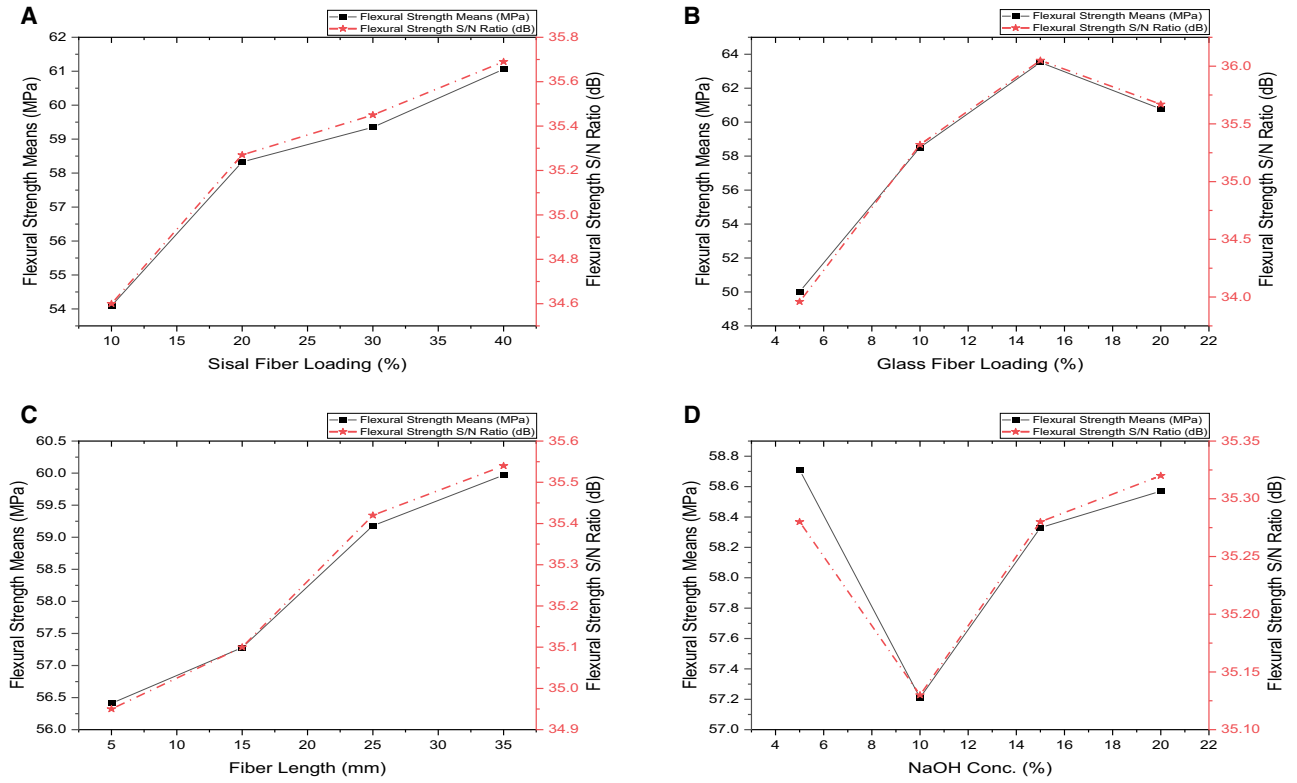

Figure 4. (**A**) Effect of sisal fiber loading on the flexural strength of the developed composite. (**B**) Effect of glass fiber loading on the flexural strength of the developed composite. (**C**) Effect of fiber length on the flexural strength of the developed composite. (**D**) Effect of NaOH concentration on the flexural strength of the developed composite.

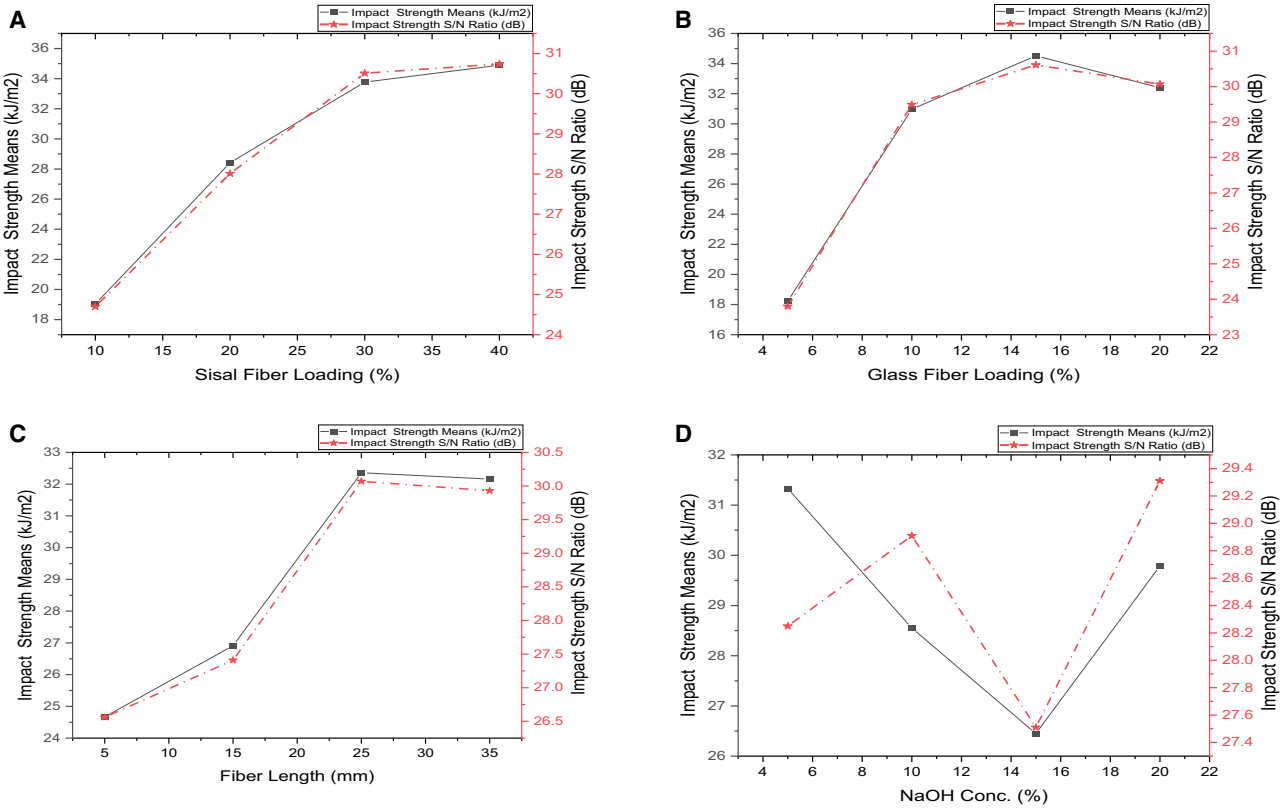

Figure 5. (**A**) Effect of sisal fiber loadings on the impact strength of the developed composite. (**B**) Effect of glass fiber loadings on the impact strength of the developed composite. (**C**) Effect of fiber length on the impact strength of the developed composite. (**D**) Effect of NaOH concentration on the impact strength of the developed composite.

Analysis of variance for the single objective optimization

Table 6 presents the analysis of the variance of the different factors on the measured effects, which was carried out at a 95% confidence level. It was observed that the sisal and glass fiber loading had a significant effect on the tensile strength of the material with P-values of 0.003 and 0.016, which were less than 0.05. The percentage contribution of the sisal fiber loading to the tensile strength of the material was observed to be 70.29%. The difference between the percentage contribution of sisal and glass fiber may not only be due to the volume difference but also that the sisal fiber is known to have a considerable strength of 350 MPa [94]. All the factors under consideration (sisal fiber loading, glass fiber loading, fiber length, and NaOH treatment concentration) have a significant influence on the flexural strength of the material developed for aircraft body application, with P-values all less than 0.05. The percentage contribution of glass fiber loading to the flexural strength of the material was observed to be the highest at 73.88%, with sisal fiber loading at 19.12%. The influence of sisal fiber loading and glass fiber loading was also observed to be significant on the impact strength of the material, with P-values of 0.027 and 0.026, respectively, and percentage contributions of 40.62 and 41.81%, respectively. This fiber reinforcement increases the impact strength of the matrix, which has a lower impact energy. Moreso, the length of the fiber determines the surface area with which bonding with the matrix takes place. The larger the bonding area, the more strength is needed for general fiber debonding or pulling out. Also, the sisal fiber loading, glass fiber loading, and fiber length were observed to have a significant influence on the density of the material. The NaOH concentration was observed to have no significance on the density with a P-value of 0.428, less than 0.05. This implies that a reduction of the sisal fiber, glass fiber, or fiber length in the composites, when used in the development of aircraft, will significantly affect the carbon emission of the aircraft. Important to note also is that the process of producing glass fibers incurs more carbon emissions or global heating than the production of fibers from natural sources.

Interaction plots for the effect of sisal fiber loading and glass fiber loading on the tensile, flexural, impact energy, and density of the materials are presented in Fig. 7A–D. Figure 7A(i) and (ii) showed a significant interaction between the sisal fiber loading and the glass fiber loading on the tensile strength of the material. It was observed that the tensile strength was optimum when sisal fiber loading was between 15–30% and the glass fiber loading was between 7–12% glass fiber loading. Low tensile strength was observed at low sisal fiber loading and high glass fiber loading. Figure 7B(i) and (ii) show that the interaction of the sisal fiber loading and the glass fiber loading was significant on the flexural strength at 15–25% and 6–12%, respectively. Sisal fiber possesses more elastic properties than glass fiber, which is brittle due to its crystalline properties. Moreso, Fig. 7C(i) and (ii) also show that the interaction between the fiber loading yields significant differences in the impact strength of the material. The highest impact strength was obtained at sisal fiber loadings beyond 20%. Figure 7D(i) and (ii) also show that variations in the sisal fiber loading and glass fiber loading have a significant effect on the density of the material. Materials developed for aircraft structures must be light in weight, and therefore, to achieve this, a lesser quantity of more dense materials like glass fiber is needed with more quantities of the natural fibers (sisal) needed

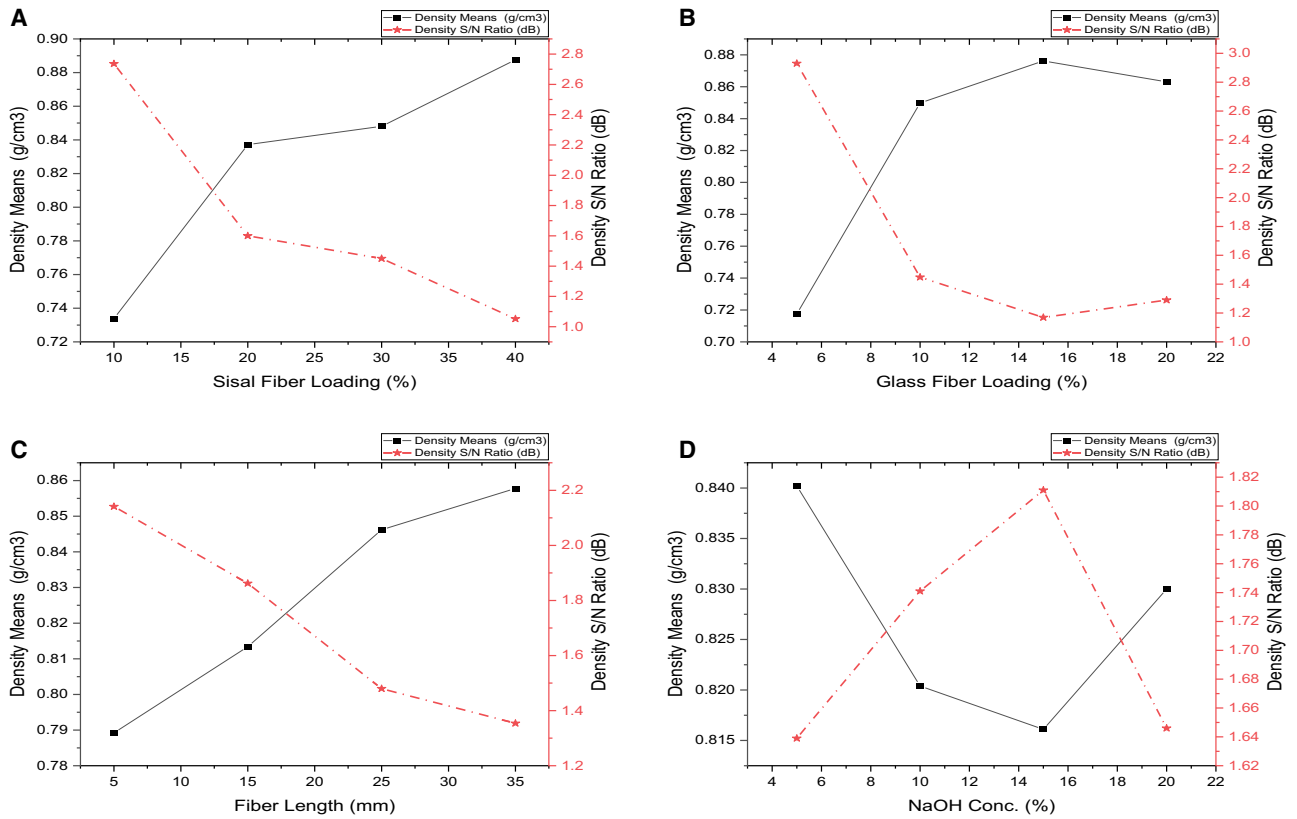

Figure 6. (**A**) Effect of sisal fiber loadings on the density of the developed composite. (**B**) Effect of glass fiber loadings on the density of the developed composite. (**C**) Effect of fiber length on the density of the developed composite. (**D**) Effect of NaOH concentration on the density of the developed composite.

as well. This is even beneficial to the environment, as natural fibers are biodegradable, and the application of more natural fibers in the development of aircraft structures aligns with sustainable policies.

Single objective optimization

Table 7 presents the optimal combinations of the process parameters to obtain the best performance for the individual effects. It shows that the developed material for aircraft body application has an optimally confirmed tensile strength of 80.1 MPa at a 20% sisal fiber loading, a 15% glass fiber loading, a 25 mm fiber length, and a NaOH concentration of 10% for the fiber treatment. This is commendably higher when compared to the tensile strength of other fiber-reinforced polymer composites, as in [95], with 24.5 MPa as the best tensile performance. Also, a sisal fiber loading of 40%, a glass fiber loading of 15% at a fiber length of 35 mm, and a NaOH treatment concentration of 5% delivered the best flexural strength of 68.3 MPa. This falls within range when compared to the flexural strength of sisal/kevlar hybrid composites that were further filled with particulate reinforcement and had a flexural strength of 76.97 MPa. Moreso, the process parameter combination of sisal fiber loading, glass fiber loading, a fiber length of 25 mm, and a NaOH concentration of 35% produced the best impact strength of 39.7 kJ/m^2. Materials designed for aircraft application, particularly skin (body) materials, are expected to be tough having a high impact strength to withstand circumstances such as bird strikes or impacts during conveyance. The weight of the composite developed with sisal fiber loading at 10%, glass fiber loading at 5%, fiber length at 5 mm, and NaOH concentration at 15% produced the lowest density. It was observed that the density of the obtained material was significantly reduced at the optimal combination. The reduction in the density of materials for aircraft applications directly reduces operational costs and carbon emissions. That is why the aviation industry, beyond structural reliability, has advocated for lightweight materials. Even though the presence of reinforcement, particularly in treated natural fiber composites, may directly result in a reduction in the weight of the material, a possible drawback will be the formation of pores, either due to the randomness of the fibers in the matrix or due to the production process. Although the formation of voids (pores) in the material may be a disadvantage to its structural reliability in that the voids may act as localized centers of crack initiation, they can also be advantageous depending on their shapes, can also act as localized points of crack mitigation. Figure 8A and B shows the SEM image of the combination of run 2 (lowest performing) and the best performing combination as with the grey relational analysis. The nature of the voids discovered in the developed composite, which were circular and oval shapes, position them as a crack mitigator more than as a defect. It was also observed that the worst performing had more voids as presented in Fig. 8A and the best performing had less voids as represented in Fig. 8B. The best-performing material likely had better interfacial bonding between the fibers and the epoxy matrix. Enhanced adhesion prevents the formation of voids and delamination during loading, resulting in fewer pores and a smoother fracture surface.

Regression analysis on single objective optimization

The tensile, flexural, impact, and density properties of the material were modeled using regression analysis. The obtained

Table 6. Analysis of variance on the means of tensile, flexural, impact strength, and density of the developed material

		Tensile strength					
Source	**DF**	**Seq SS**	**Adj SS**	**Adj MS**	***F***	***P***	**% Cont.**
Sisal fiber loading (%)	3	823.06	823.058	274.353	63.71	0.003	70.29
Glass fiber loading (%)	3	270.77	270.77	90.257	20.96	0.016	23.12
Fiber length (mm)	3	60.61	60.613	20.204	4.69	0.118	5.18
NaOH conc. (%)	3	3.66	3.657	1.219	0.28	0.836	0.31
Residual error	3	12.92	12.918	4.306			1.10
Total	15	1171.02					100.00
		Flexural strength					
Source	**DF**	**Seq SS**	**Adj SS**	**Adj MS**	***F***	***P***	**% Cont.**
Sisal fiber loading (%)	3	105.479	105.479	35.16	241.28	0	19.12
Glass fiber loading (%)	3	407.473	407.473	135.824	932.09	0	73.88
Fiber length (mm)	3	32.585	32.585	10.862	74.54	0.003	5.91
NaOH conc. (%)	3	5.572	5.572	1.857	12.75	0.033	1.01
Residual error	3	0.437	0.437	0.146			0.08
Total	15	551.545					100.00
		Impact strength					
Source	**DF**	**Seq SS**	**Adj SS**	**Adj MS**	***F***	***P***	**% Cont.**
Sisal fiber loading (%)	3	627.87	627.87	209.29	14.66	0.027	40.62
Glass fiber loading (%)	3	646.3	646.3	215.43	15.09	0.026	41.81
Fiber length (mm)	3	177.52	177.52	59.17	4.15	0.137	11.49
NaOH conc. (%)	3	51.11	51.11	17.04	1.19	0.444	3.31
Residual error	3	42.82	42.82	14.27			2.77
Total	15	1545.62					100.00
		Density					
Source	**DF**	**Seq SS**	**Adj SS**	**Adj MS**	***F***	***P***	**% Cont.**
Sisal fiber loading (%)	3	0.051584	0.051584	0.017195	47.15	0.005	39.48
Glass fiber loading (%)	3	0.064879	0.064879	0.021626	59.3	0.004	49.66
Fiber length (mm)	3	0.011719	0.011719	0.003906	10.71	0.041	8.97
NaOH conc. (%)	3	0.001376	0.001376	0.000459	1.26	0.428	1.05
Residual error	3	0.001094	0.001094	0.000365			0.84
Total	15	0.130651					100.00

Table 7. Optimal combinations for the various effects

S/N	**Effects**	**Optimum combination**				**Predicted Opt. effect**	**Confirmed Opt. effect**	**Diff.**	**Con. Int.**	**% Error**
		A	**B**	**C**	**D**					
1.	Tensile Strength	20%	15%	25 mm	10%	82.36 MPa	80.1 MPa	2.26 MPa	±5.134 MPa	2.74
2.	Flexural Strength	40%	15%	35 mm	5%	68.6 MPa	68.3 MPa	0.3 MPa	±0.95 MPa	0.44
3.	Impact Strength	40%	15%	25 mm	35%	46.1 kJ/m^2	39.7 kJ/m^2	6.4 kJ/m^2	±9.35 kJ/m^2	13.88
4.	Density	10%	5%	5 mm	15%	0.5765g/cm^3	0.5701g/cm^3	0.0064g/cm^3	0.0473g/cm^3	1.11

models were used for the prediction of the various properties of the materials at different possible combinations of the process parameters. Models are presented in Equations (17–20). Also, excellent R-Square values were obtained, which speaks to the high reliability of the models in predicting the mechanical properties of the material. The measures of accuracy of the models for the tensile strength, flexural strength, and impact strength are observed to be commendable with R-Squared values of 88.79%, 81.13%, and 82.84% respectively. It was also observed that the density model, which directly translates to the carbon emission of the aircraft, had a high prediction accuracy of 89.12%.

$$\text{Tensile Strength (MPa)} = 62.0 + 0.425\ A - 1.437\ B + 1.404\ C - 0.937\ D - 0.0519\ B*C + 0.1481\ B*D - 0.0476\ C*D \quad (17)$$

$$\text{Flexural Strength (MPa)} = 53.80 + 0.1636\ A - 0.745\ B + 0.473\ C + 0.569\ D - 0.0278\ C*D \quad (18)$$

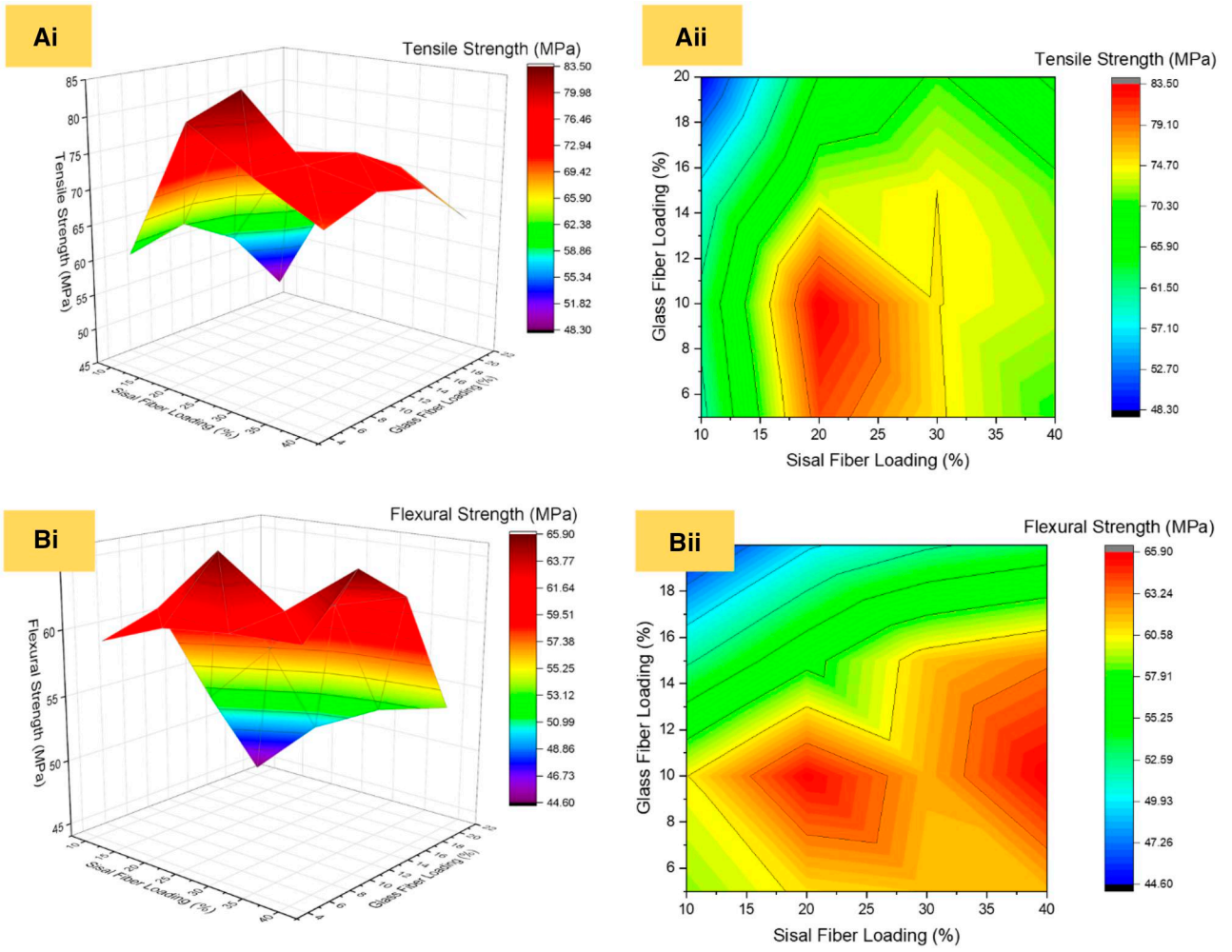

Figure 7. (**A**) (i) 3D interaction plot for sisal fiber loading and glass fiber loading on the tensile strength of the material. (ii) 2D contour plot for sisal fiber loading and glass fiber loading interaction on the tensile strength of the material. (B) (i) 3D interaction plot for sisal fiber loading and glass fiber loading on the flexural strength of the material. (ii) 2D contour plot for sisal fiber loading and glass fiber loading interaction on the flexural strength of the material. (**C**) (i) 3D interaction plot for sisal fiber loading and glass fiber loading on the Impact strength of the material. (ii) 2D contour plot for sisal fiber loading and glass fiber loading interaction on the Impact strength of the material. (**D**) (i) 3D interaction plot for sisal fiber loading and glass fiber loading on the density of the material. (ii) 2D contour plot for sisal fiber loading and glass fiber loading interaction on the density of the material.

$$\text{Impact Strength } (\text{kJ/m}^2) = 26.4 + 0.437\ \text{A} - 1.621\ \text{B} + 0.680\ \text{C} - 0.194\ \text{D} + 0.0561\ \text{B} * \text{D} - 0.0321\ \text{C} * \text{D} \quad (19)$$

$$\text{Density } (\text{g/cm}^3) = 0.611 + 0.00526\ \text{A} - 0.00591\ \text{B} + 0.01294\ \text{C} + 0.00487\ \text{D} - 0.000367\ \text{B} * \text{C} + 0.000319\ \text{B} * \text{D} - 0.000477\ \text{C} * \text{D} \quad (20)$$

Grey relational analysis

Grey relational analysis is a statistical tool that was applied to obtain the optimum point at which carbon emissions through the weight of the material can be at their lowest (best minimum) while the structural reliability (tensile, flexural, and impact strength) is at its highest possible (best maximum). Generally, it was applied to obtain the best composition of the manufacturing parameters of the composite in which there is the lowest carbon emission at the best structural reliability. Table 8 presents the normalization of the means for the measured effect, while and also shows the deviation sequence from unity (1). Furthermore, it shows the obtained gray relational coefficient, the gray relational grade, and the ranks for each. Having the highest rank, it is observed that run 7 has a process parameter combination of sisal fiber loading at 20%, glass fiber loading at 10%, fiber length at 35 mm, and 5% NaOH. Also, the general mean was obtained at 0.5894. The response table for the gray relational grades is presented in Table 9. It is observed that glass fiber loading has the highest influence on the mechanical properties of materials for the development of aircraft structures. This is not dissociated from the high mechanical properties of the glass fibers due to their crystalline nature. The sisal fiber, having a rank of two and a delta of 0.1311, had the second greatest influence on the mechanical properties of the material in its design for aircraft application. Figure 9A–D shows the effect of the various process parameters on the grey relational grade (potential for application as aircraft material).

Figure 9A shows that the sisal fiber loading has a positive influence on the gray relational grade between 10 and 20%. That is, sisal is a factor of positive effect on the development of aircraft to achieve low emissions with good structural reliability. Beyond this, the influence is less significant, and less change is seen. This implies that in the development of materials for aircraft structures, sisal fibers can effectively replace the volume

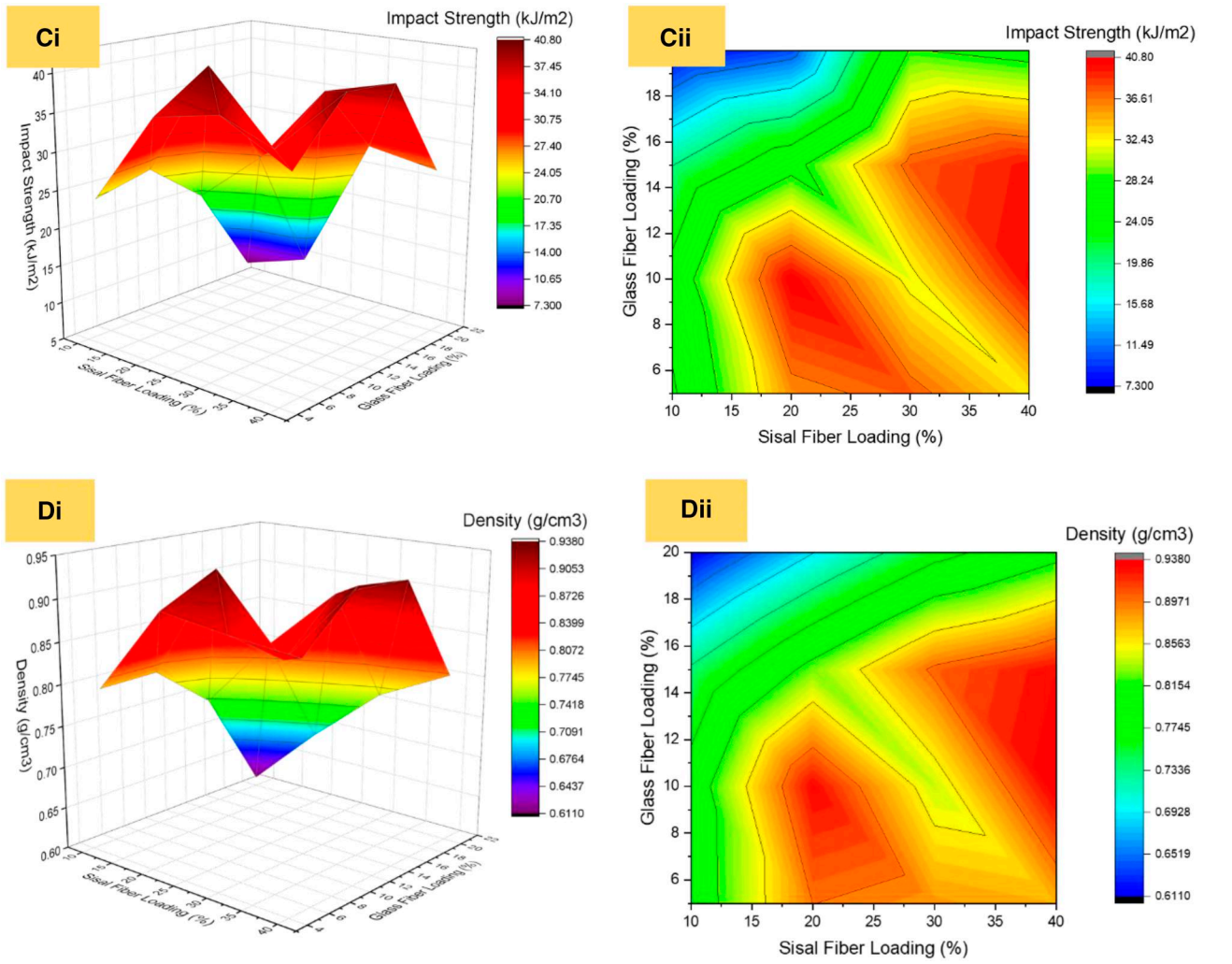

Figure 7. Continued.

percentage of glass fiber and still give significant structural reliability.

Figure 9B shows that glass fiber, due to its good mechanical properties, generally has a positive influence on the design of materials for the development of aircraft structures. Although this positive influence was observed to decline at glass fiber loadings beyond 15%, this may be a result of deleterious microstructure formations like voids developing in the material. This implies that at lower glass fiber loadings, the materials tend to be more suitable for the reduction of carbon emissions because of their weight. But at higher glass fiber loading, the weight of the material increases, leading to an increase in fuel consumption and carbon emissions.

Generally, increasing the fiber length of reinforcement improves the applicability of the natural fiber hybrid composite in aircraft structures, as observed in Fig. 9C. It reduces the carbon emissions of the aircraft. Even from the manufacturing point of view, the energy used in the production of short-fiber composites is higher than the energy used in the production of longer-fiber composites due to the increased processes. The best-performing grey relational grade was observed at fiber lengths of 35 mm. The linear behavior makes it evident that a fiber length of more than 35% will also increase the performance of the material.

According to Fig. 9D, it is observed that between the range of NaOH concentrations of 5–10%, the performance of the material for the development of aircraft structures reduces. This may be due to the removal of lignin from the surface of the fibers, leaving a rather smooth surface that may still have poor interfacial adhesion with the matrix material. But beyond the NaOH concentration of 10%, the performance of the material increases. This is due to the proper alkalization of the surface of the fibers, which results in a rough surface and proper interfacial adhesion.

Analysis of variance for the grey relational grade

Table 10 presents the analysis of the variance of the means for the gray relational grade. At a 95% confidence level (*P*-value = 0.05), it was observed that the fiber length had the most significant influence on the grey relational grades with a *P*-value of 0.004, which is less than 0.05. This implies that the length of the fibers used in the development of polymer composite materials for aircraft structures can determine their performance to a large extent. It can be a strong determinant of the carbon emission of the aircraft. Also, the percentage contribution of the fiber length to the performance of the grey relational grades was 34.19%. The fiber length of the glass fiber was also observed to be significant for the performance of the material in the targeted application, as it had a *P*-value of 0.017 and a percentage contribution of 18.04%. The interaction of sisal fiber loading and glass fiber loading on the grey relational grades is shown graphically on 3D and

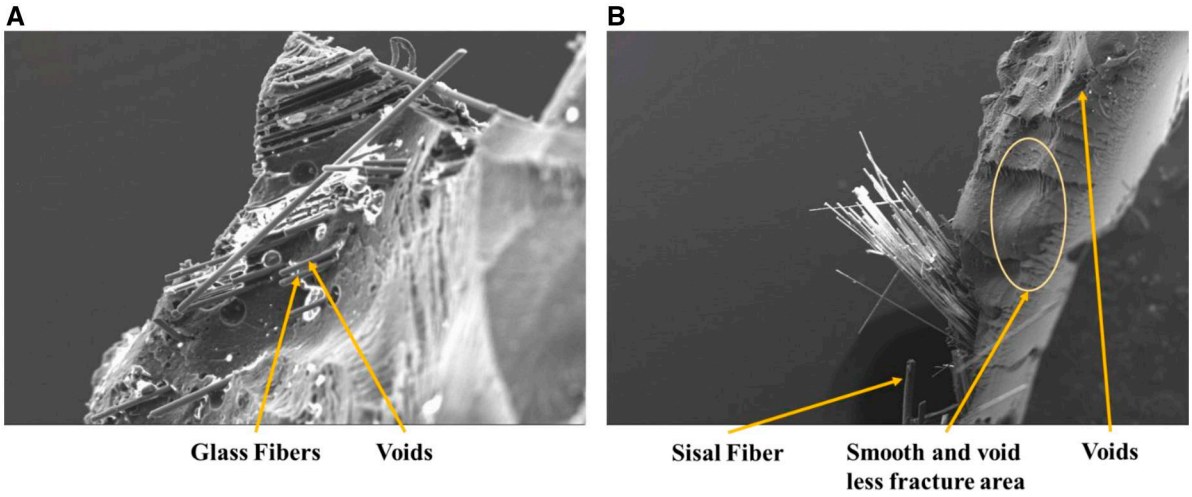

Figure 8. SEM image on (**A**) worst performing composite material, (**B**) best performing (optimum) composite material.

Table 8. Effect normalization of the tensile, flexural, impact, and densities of the developed composite

S/N	Normalization				Deviation sequence				Grey relational coefficient				Grey relational grades	Ranks
	Tensile Strength	Flexural Strength	Impact Strength	Density	Tensile Strength	Flexural Strength	Impact Strength	Density	Tensile Strength	Flexural Strength	Impact Strength	Density		
1	0.0000	0.0000	0.0000	1.0000	1.0000	1.0000	1.0000	0.0000	0.3333	0.3333	0.3333	1.0000	0.5000	13
2	0.2760	0.3572	0.3721	0.6108	0.7240	0.6428	0.6279	0.3892	0.4085	0.4375	0.4433	0.5623	0.4629	16
3	0.4045	0.7487	0.5438	0.4415	0.5955	0.2513	0.4562	0.5585	0.4564	0.6655	0.5229	0.4724	0.5293	10
4	0.3434	0.6770	0.4863	0.4463	0.6566	0.3230	0.5137	0.5537	0.4323	0.6075	0.4932	0.4745	0.5019	12
5	0.5053	0.2312	0.0854	0.7542	0.4947	0.7688	0.9146	0.2458	0.5027	0.3941	0.3535	0.6704	0.4801	15
6	0.7051	0.5927	0.5880	0.3380	0.2949	0.4073	0.4120	0.6620	0.6290	0.5511	0.5482	0.4303	0.5397	9
7	1.0000	0.9910	1.0000	0.0166	0.0000	0.0090	0.0000	0.9834	1.0000	0.9824	1.0000	0.3371	0.8299	1
8	0.9178	0.7673	0.8519	0.1233	0.0822	0.2327	0.1481	0.8767	0.8588	0.6824	0.7715	0.3632	0.6690	3
9	0.6395	0.3587	0.6326	0.5360	0.3605	0.6413	0.3674	0.4640	0.5810	0.4381	0.5764	0.5187	0.5286	11
10	0.7508	0.7987	0.9009	0.1084	0.2492	0.2013	0.0991	0.8916	0.6674	0.7130	0.8345	0.3593	0.6435	6
11	0.7536	0.8223	0.7296	0.2954	0.2464	0.1777	0.2704	0.7046	0.6699	0.7378	0.6490	0.4151	0.6180	7
12	0.7616	0.7952	0.9043	0.1586	0.2384	0.2048	0.0957	0.8414	0.6772	0.7094	0.8393	0.3727	0.6497	5
13	0.4767	0.4247	0.5880	0.4079	0.5233	0.5753	0.4120	0.5921	0.4886	0.4650	0.5482	0.4578	0.4899	14
14	0.6600	0.8683	0.9708	0.0201	0.3400	0.1317	0.0292	0.9799	0.5952	0.7916	0.9448	0.3379	0.6674	4
15	0.7045	1.0000	0.9841	0.0000	0.2955	0.0000	0.0159	1.0000	0.6286	1.0000	0.9692	0.3333	0.7328	2
16	0.6295	0.8046	0.7597	0.1863	0.3705	0.1954	0.2403	0.8137	0.5744	0.7190	0.6754	0.3806	0.5873	8
												Mean	0.5894	

Table 9. Mean and S/N ratio response table for grey relational grades

Levels	Grey relational grade							
	Sisal fiber loading (%)		Glass fiber loading (%)		Fiber length (mm)		NaOH conc. (%)	
	Mean	S/N Ratio (dB)	Mean	S/N Ratio (dB)	Mean	S/N Ratio (dB)	Mean	S/N Ratio (dB)
1	0.4985	−6.056	0.602	−4.462	0.5612	−5.045	0.6617	−3.725
2	0.6297	−4.21	0.6775	−3.507	0.5814	−4.877	0.5599	−5.14
3	0.6099	−4.323	0.5784	−4.847	0.5986	−4.517	0.5601	−5.087
4	0.6194	−4.258	0.4997	−6.032	0.6163	−4.408	0.5757	−4.896
Delta	0.1311	1.846	0.1778	2.525	0.0551	0.637	0.1018	1.415
Rank	2	2	1	1	4	4	3	3

2D contour plots in Fig. 10A(i) and (ii). It shows that the best GRG (best performance of the material on its applicability on aircraft) was at sisal fiber loading between 15 and 25% and glass fiber loading between 8 and 12%. More so, Fig. 10B(i) and (ii) presents the relationship between sisal fiber loading and the NaOH concentration for treatment. It shows that the best GRG performance was between a sisal fiber loading of 15 and 25%.

Optimization and confirmation of the grey relational grades

The grey relational grades were optimized for the higher, the better. From the grey relational grade response tables, it was observed that the best performance was at a process parameter combination of 20% sisal fiber loading, 15% glass fiber loading, fiber length at 35 mm, and NaOH concentration at 5%. The

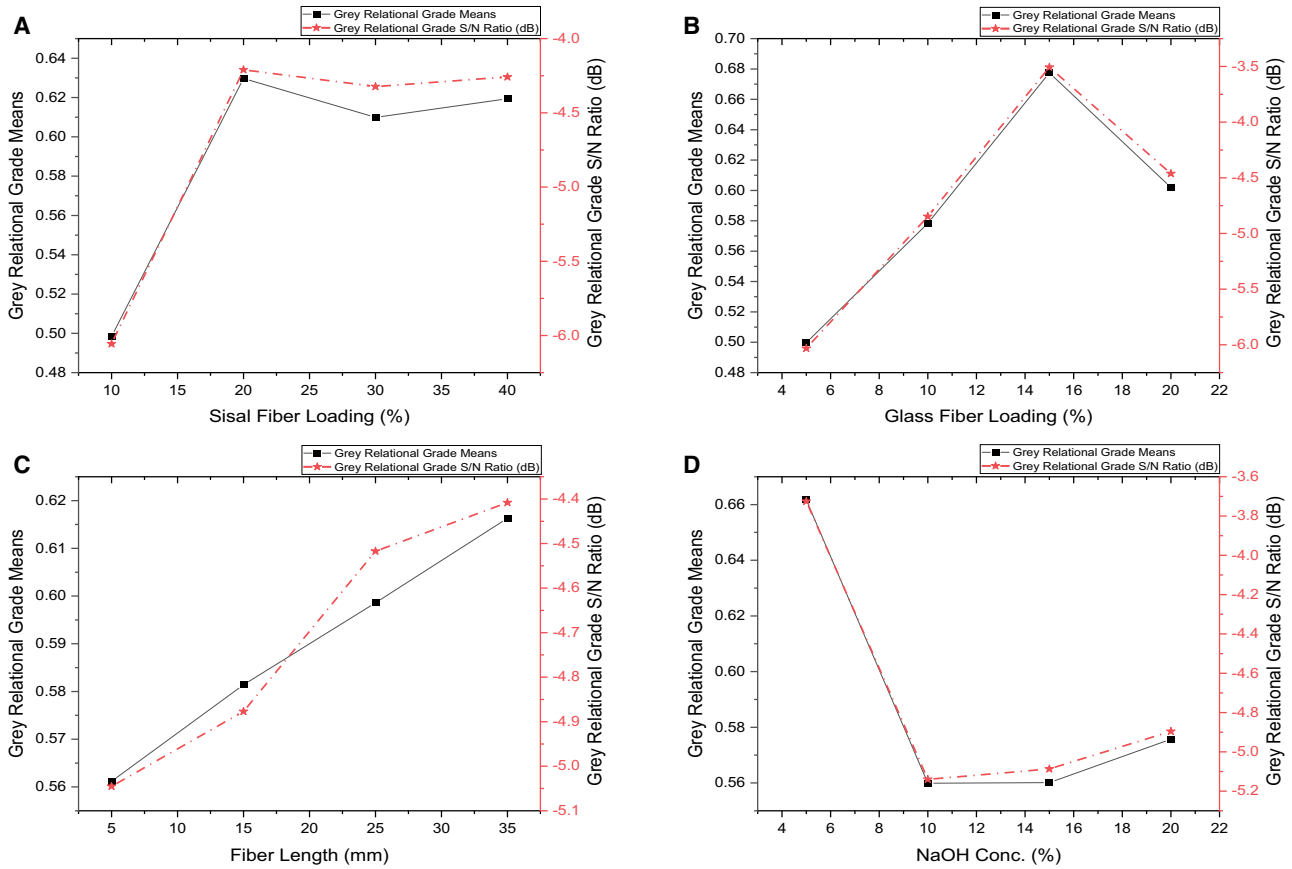

Figure 9. (**A**) Effect of sisal fiber loading on the grey relational grade. (**B**) Effect of glass fiber loading on the grey relational grade. (**C**) Effect of fiber length loading on the grey relational grade. (**D**) Effect of fiber length loading on the grey relational grade.

obtained GRG average at these levels was 0.6297, 0.6775, 0.6163, and 0.6617, respectively. Using Equation (8), the optimum grey relational grade was predicted to be 0.817. The confirmation of the prediction was carried out by developing the composite materials at the optimum parameter combination. The obtained tensile, flexural, impact, and density at the optimum combination were 83.43 MPa, 65.84 MPa, 43.5 kJ/m^2, and 0.8400 g/cm^3 respectively. The obtained GRG for the confirmation experiment was 0.7005. The difference between the confirmation and the predicted optimum grey relational grade agrees with the confidence interval of 0.0891 obtained from Equation (9).

Regression analysis and modeling of the grey relational grades

The grey relational grade was modeled using regression analysis. The obtained model is presented in Equation (21). R-Sq of 88.19% and R-Sq adjusted of 74.69% show relatively good reliability in the model predicting the applicability of the materials in aircraft based on the combination of the parameters studied, which are sisal fiber loading, glass fiber loading, fiber length, and NaOH concentration.

$$\begin{aligned} GRG = {} & 0.427 - 0.00056A + 0.00435B + 0.02374C - 0.0200D \\ & + 0.000624\ A*D - 0.001151\ B*C \\ & + 0.000745\ B*D - 0.000502\ C*D \end{aligned} \quad (21)$$

Machine learning (genetic algorithm)

The models derived from the regression analysis of the Taguchi orthogonal array were applied as the fitness function for the genetic algorithm. Figure 11A and B presents the best fitness and the current best fitness function for the single objective optimization of the grey model for the developed material. It is observed that the best fitness was obtained at about the 100th generation.

The fitness of one generation is usually carried on to the next generation. The respective best values (performance of the fitness function in every generation) of the tensile, flexural, impact strength, and density were obtained to be 102.55 MPa, 71.15 MPa, 54.39 kJ/m^2, and 0.6177 g/cm^3 respectively. While the best values for the fitness function for the grey relational grade was observed to be 1.0. It is observed that with the GA method, less time is taken for the computation of the best fitness (optimization) of the parameters. Also, the best combination to give the optimum performance of the developed composite for aircraft bodies using the genetic algorithm on the grey function is sisal fiber at 40%, glass fiber at 5%, fiber length at 35 mm, and NaOH concentration at 5%.

Conclusion

The genetic algorithm method of the machine learning principle was applied to optimize the process parameters for the manufacture of natural fiber-reinforced polymer composites for aircraft structural applications to reduce carbon emissions because of fuel consumption. Conclusions drawn include the fact that it is possible to develop a composite of sisal hybridized with glass fiber as a lightweight material for sustainable and low-greenhouse-emission aircraft.

Table 10. Analysis of variance on the grey relational grades means

Source	DF	Adj SS	Adj MS	*F*-value	*P*-value	% Cont.
Regression	8	0.142379	0.017797	6.53	0.011	
Sisal fiber loading (%)	1	0.000071	0.000071	0.03	0.876	0.049
Glass fiber loading (%)	1	0.000756	0.000756	0.28	0.615	0.51
Fiber length (mm)	1	0.050217	0.050217	18.44	0.004	34.19
NaOH conc. (%)	1	0.010119	0.010119	3.71	0.095	6.89
Sisal fiber loading (%) × NaOH conc. (%)	1	0.020425	0.020425	7.5	0.029	13.91
Glass fiber loading (%) × fiber length (mm)	1	0.026489	0.026489	9.72	0.017	18.04
Glass fiber loading (%) × NaOH conc. (%)	1	0.007049	0.007049	2.59	0.152	4.80
Fiber length (mm) × NaoH conc. (%)	1	0.012667	0.012667	4.65	0.068	8.63
Error	7	0.019067	0.002724			12.98
Total	15	0.161446				

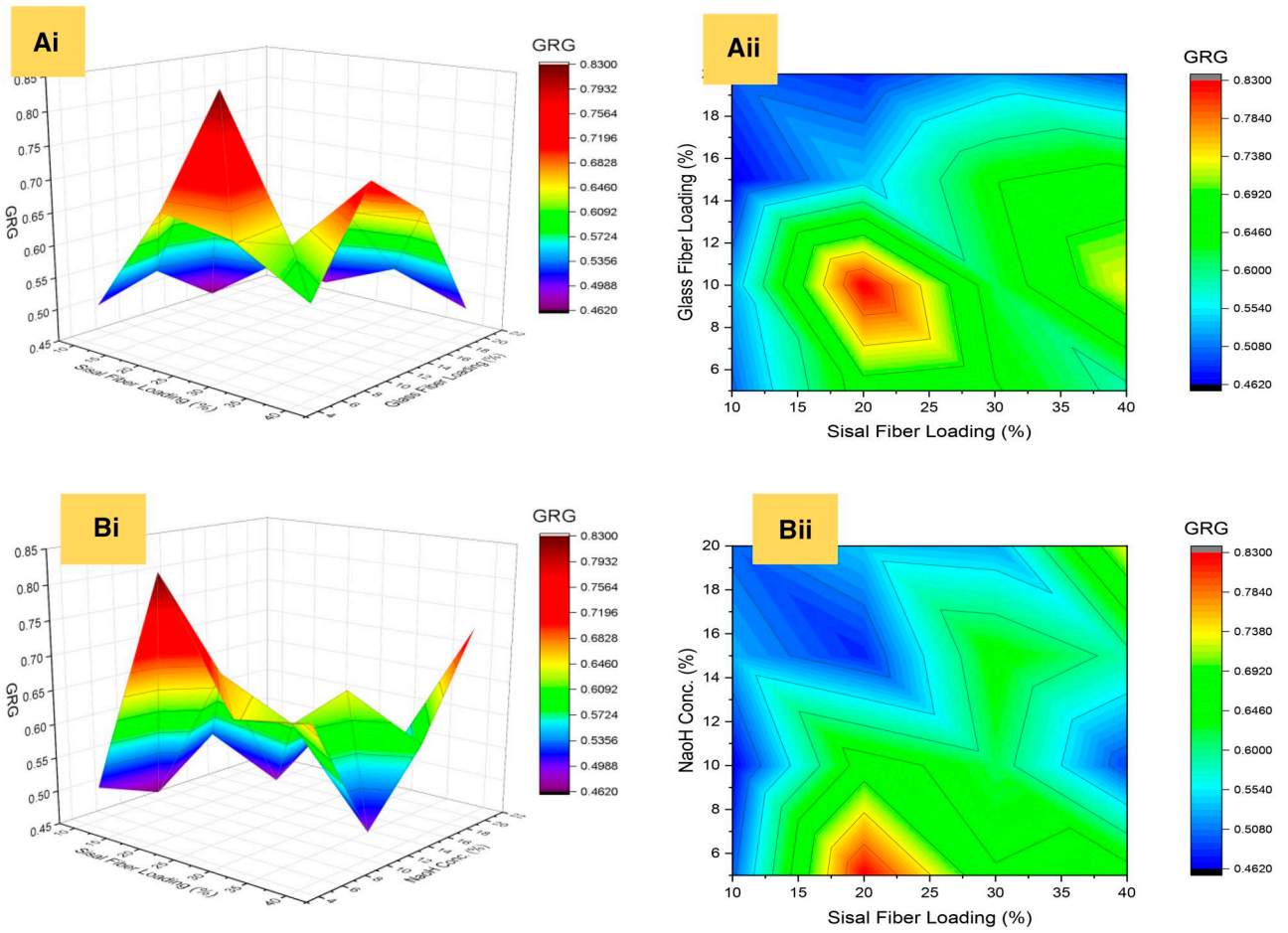

Figure 10. (**A**) (i) 3D interaction effect of sisal fiber loading and glass fiber loading on grey relational grades. (ii) 2D contour plots interaction effect of sisal fiber loading and glass fiber loading on grey relational grades. (**B**) (i) 3D interaction effect of sisal fiber loading and NaOH concentration on grey relational grades. (ii) 2D contour plot interaction effect of sisal fiber loading and NaOH concentration on grey relational grades.

The optimized tensile strength, flexural strength, impact strength, and density of the developed composites using the Taguchi single objective optimization method are 80.1 MPa, 68.3 MPa, 39.7 kg/m^2, and 0.5765 g/cm^3. The sisal fiber content, glass fiber content, fiber length, and NaOH concentration have a significant effect on the tensile strength, flexural strength, and impact strength, of the material, as revealed by the analysis of variance. Because of their weight, they are also observed to be significant in the level of carbon emissions of the aircraft. Regression models for tensile strength, flexural strength, impact strength, and density demonstrated prediction accuracy of 88.79%, 87.13%, 82.84%, and 89.12%, respectively. Multi-objective optimization with grey relational analysis showed that the best combination of process parameters for the development of materials for aircraft structures for low carbon emission is 20% sisal fiber content, 15% glass fiber loading, 35 mm fiber length, and 5% NaOH concentration. The analysis of variance on the gray relational grades shows that the sisal fiber content has a significant effect on the development of aircraft materials for low carbon emissions with a *P*-value less than 0.05 at a 95% confidence level. The genetic algorithm on the developed models showed that the optimum process parameters for the development of the hybrid

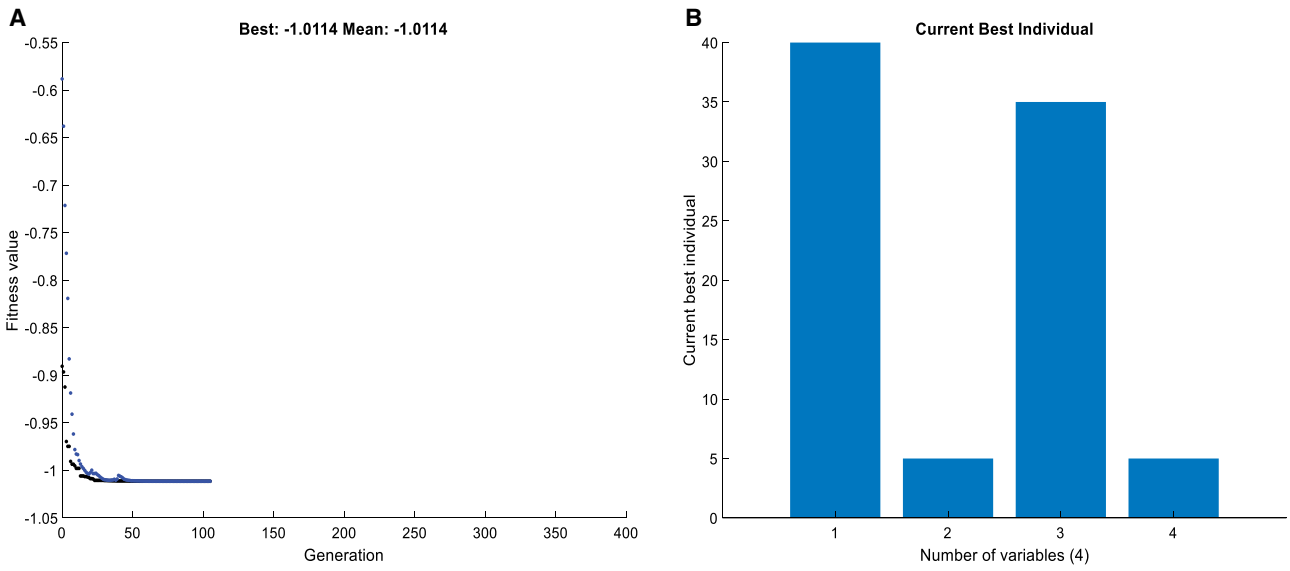

Figure 11. (**A**) GRG best fitness. (**B**) GRG current best individual.

material for low carbon emission aircraft structure are sisal fiber content at 40%, glass fiber content at 5%, fiber length at 35%, and NaOH concentration at 5%.

Importantly, this study lays the groundwork for reducing greenhouse gas emissions in the air transportation industry via the material route. Although the study of all-around sustainability (production of the whole material with no synthetic material) was not explored, it remains a gap for further studies.

Data and code availability

All data and supporting information relevant to this study are included within the main text. Any additional datasets or resources required for reproducing the findings presented in this article like the codes used for the optimization will be provided upon request.

Author Contributions

Moses Olabhele Esangbedo (Conceptualization, Formal Analysis, Funding acquisition, Investigation, Project administration, Supervision, Writing—review & editing) and Bassey Okon Samuel (Data curation, Formal Analysis, Investigation, Methodology, Project administration, Writing—original draft)

Funding

This research received no funding.

Conflict of interest statement: All authors certify that they have no affiliations with or involvement in any organization or entity with any financial interest or non-financial interest in the subject matter or materials discussed in this manuscript.

Ethics approval

Not applicable.

Consent to participate

Not applicable.

References

1. Browne M, Dubois A, Hulthén K. Transportation as a loosely coupled system: a fundamental challenge for sustainable freight transportation. *Int J Sustain Transport* 2023;**17**:804–14.
2. Transport E. *Increasing Oil Consumption and Greenhouse Gas Emissions Hamper EU Progress towards Environment and Climate Objectives*. Copenhagen, Denmark: European Environment Agency, 2020.
3. de VC, Smit S, Nilsson A, Kuramochi T. Climate targets by major steel companies: an assessment of collective ambition and planned emission reduction measures. *Energy Clim Change* 2024; **5**:100120.
4. Terrenoire E, Hauglustaine D, Gasser T, Penanhoat O. The contribution of carbon dioxide emissions from the aviation sector to future climate change. *Environ Res Lett* 2019;**14**:084019.
5. Liu Z, Deng Z, Zhu B *et al.* Global patterns of daily CO_2 emissions reductions in the first year of COVID-19. *Nat Geosci* 2022; **15**:615–20.
6. Oreggioni GD, Ferraio FM, Crippa M *et al.* Climate change in a changing world: socio-economic and technological transitions, regulatory frameworks and trends on global greenhouse gas emissions from EDGAR V. 5.0. *Glob Environ Change* 2021; **70**:102350.
7. Ng KS, Farooq D, Yang A. Global biorenewable development strategies for sustainable aviation fuel production. *Renew Sustain Energy Rev* 2021;**150**:111502.
8. Yang L, Hu Y-J, Wang H *et al.* Uncertainty quantification of CO_2 emissions from china's civil aviation industry to 2050. *J Environ Manage* 2023;**336**:117624.
9. Lazic D, Grujic V, Cvetkovic D. Results of using sustainable aviation fuel in transport aircraft on different flight levels and their influence on carbon-dioxide Co2 emissions. *Zeszyty Naukowe. Transport/Politechnika l ska* 2023.
10. Paz J. Global energy outlooks and australia's net zero energy future. *Appea J* 2022;**62**:S63–S66.
11. DeAngelo J, Azevedo I, Bistline J *et al.* Energy systems in scenarios at net-zero CO2 emissions. *Nat Commun* 2021;**12**:6096.
12. Brecha RJ, Ganti G, Lamboll RD *et al.* Institutional decarbonization scenarios evaluated against the paris agreement 1.5 C goal. *Nat Commun* 2022;**13**:4304.

13. Adun H, Ampah JD, Bamisile O *et al.* Ambitious near-term decarbonization and direct air capture deployment in Latin America's net-zero goal. *Energy Sustain Dev* 2023;**77**:101338.
14. Dray L, Schäfer AW, Grobler C *et al.* Cost and emissions pathways towards net-zero climate impacts in aviation. *Nat Clim Chang* 2022;**12**:956–62.
15. Apostolidis A. Decarbonizing by 2050: optimists, pessimists and realists. *Aerosp Am* 2021;**59**:40–2.
16. Bills A, Sripad S, Fredericks WL *et al.* Performance metrics required of next-generation batteries to electrify commercial aircraft. *ACS Energy Lett* 2020;**5**:663–8.
17. Johnson W, Silva C. NASA concept vehicles and the engineering of advanced air mobility aircraft. *Aeronaut J* 2022;**126**:59–91.
18. Barzkar A, Ghassemi M. Electric power systems in more and all electric aircraft: a review. *Ieee Access* 2020;**8**:169314–32.
19. Goritiyal C, Bairolu A, Goritiyal L. Application of emerging technologies in aviation MRO sector to optimize cost utilization: the Indian case. *Intell Sustain Syst* 2021;**2**:161–76.
20. Liu H, Guo Y, Zhou Y *et al.* Multifunctional nickel coated carbon fiber veil for improving both fracture toughness and electrical performance of carbon fiber/epoxy composite laminates. *Polymer Composites* 2021;**42**:5335–47.
21. Blanco D, Rubio EM, Lorente-Pedreille RM, Sáenz-Nuño MA. Lightweight structural materials in open access: latest trends. *Materials* 2021;**14**:6577.
22. Meissner R, Rahn A, Wicke K. Developing prescriptive maintenance strategies in the aviation industry based on a discrete-event simulation framework for post-prognostics decision making. *Reliab Eng Syst Saf* 2021;**214**:107812.
23. Dhara A, Lal JM. Sustainable technology on aircraft design: a review. In: *IOP Conference Series: Earth and Environmental Science*, 2021.
24. Unnikrishnan T, Kavan P. A Review Study in Ultrasonic-welding of Similar and Dissimilar Thermoplastic Polymers and Its Composites. *Materials Today: Proceedings* 2022;**56**:3294–300.
25. Meys R, Kätelhön A, Bachmann M *et al.* Achieving Net-zero Greenhouse Gas Emission Plastics by a Circular Carbon Economy. *Science* 2021;**374**:71–6.
26. Lindstad E, Lagemann B, Rialland A *et al.* Reduction of maritime GHG emissions and the potential role of E-fuels. *Transport Res D* 2021;**101**:103075.
27. Abrantes I, Ferreira AF, Silva A, Costa M. Sustainable aviation fuels and imminent technologies-CO2 emissions evolution towards 2050. *J Clean Prod* 2021;**313**:127937.
28. Parveez B, Kittur M, Badruddin IA *et al.* Scientific advancements in composite materials for aircraft applications: a review. *Polymers* 2022;**14**:5007.
29. Shahruzzaman M, Hossain S, Kabir SF *et al.* Properties and characterization of advanced composite materials. In: Pandey, L.M., Hasan, A. (eds) *Nanoscale Engineering of Biomaterials: Properties and Applications*. Singapore: Springer, 2022, 589-617. https://doi.org/10.1007/978-981-16-3667-7_21.
30. Deka N, Bera A, Roy D, De P. Methyl methacrylate-based copolymers: recent developments in the areas of transparent and stretchable active matrices. *ACS Omega* 2022;**7**:36929–44.
31. Wong JC, Ngoi KH, Chia CH *et al.* Surface hardness and abrasion resistance natures of thermoplastic polymer covers and windows and their enhancements with curable tetraacrylate coating. *Polymer* 2022;**239**:124419.
32. Ordu M, Der O. Polymeric materials selection for flexible pulsating heat pipe manufacturing using a comparative hybrid MCDM approach. *Polymers* 2023;**15**:2933.
33. Xian G, Guo R, Li C. Combined effects of sustained bending loading, water immersion and fiber hybrid mode on the mechanical properties of carbon/glass fiber reinforced polymer composite. *Composite Structures* 2022;**281**:115060.
34. Fernandes RR, Tamijani AY, Al-Haik M. Mechanical characterization of additively manufactured fiber-reinforced composites. *Aerosp Sci Technol* 2021;**113**:106653.
35. Sherwani S, Zainudin E, Sapuan S *et al.* Mechanical Properties of Sugar palm (Arenga Pinnata Wurmb. Merr)/glass fiber-reinforced poly (lactic acid) hybrid composites for potential use in motorcycle components. *Polymers* 2021;**13**:3061.
36. Pham DD, Cho J. Low-energy catalytic methanolysis of poly (ethyleneterephthalate). *Green Chem* 2021;**23**:511–25.
37. Naik V, Kumar M, Kaup V. A review on natural fiber composite material in automotive applications. *Eng Sci* 2021;**18**:1–10.
38. Karimah A, Ridho MR, Munawar SS *et al.* A review on natural fibers for development of eco-friendly bio-composite: characteristics, and utilizations. *J Mater Res Technol* 2021;**13**:2442–58.
39. Roy K, Debnath SC, Pongwisuthiruchte A, Potiyaraj P. Recent advances of natural fibers based green rubber composites: properties, current status, and future perspectives. *J Appl Polym Sci* 2021;**138**:50866.
40. Andreev O. Resource-efficient use of hydrocarbon raw materials as a factor in the transition to a 'green' economy. In: *International Scientific Conference on Agricultural Machinery Industry 'Interagromash'*, Springer International Publishing 2022, 1442–1452.
41. Kumar A, Sharma K, Dixit AR. A review of the mechanical and thermal properties of graphene and its hybrid polymer nanocomposites for structural applications. *J Mater Sci* 2019;**54**:5992–6026.
42. Yadav V, Singh S, Chaudhary N *et al.* Dry sliding wear characteristics of natural fibre reinforced poly-lactic acid composites for engineering applications: fabrication, properties and characterizations. *J Mater Res Technol* 2023;**23**:1189–203.
43. Verma D, Senal I. Natural fiber-reinforced polymer composites: feasibility study for sustainable automotive industries. In: *Biomass, Biopolymer-based Materials, and Bioenergy*. Woodhead Publishing 2019, 103–22.
44. Kaushik V, Sharma P, Priyanka P, Mali H. Numerical modeling of fiber reinforced polymer textile composites for characterizing the mechanical behavior: a review. *Materialwissenschaft Werkst* 2022;**53**:1263–89.
45. Samuel BO, Sumaila M, Dan-Asabe B. Modeling and optimization of the manufacturing parameters of a hybrid fiber reinforced polymer composite P X G Y E Z. *Int J Adv Manuf Technol* 2022;1–12.
46. Prem KR, Muthukrishnan M, Felix SA. Effect of hybridization on natural fiber reinforced polymer composite materials: a review. *Polym Compos* 2023;**44**:4459–79.
47. Kastratović G, Grbović A, Sedmak A *et al.* Composite material selection for aircraft structures based on experimental and numerical evaluation of mechanical properties. *Procedia Struct Integr* 2021;**31**:127–33.
48. Teles F, Antunes F. Novel ranking framework for retrospective simultaneous assessment of fire and mechanical performances of natural fiber reinforced polymeric composites: literature update from the previous decade. *Vinyl Addit Technol* 2022;**28**:579–90.
49. Gasman L. Additive aerospace considered as a business. In: *Additive Manufacturing for the Aerospace Industry*. Elsevier, 2019, 327-40. https://doi.org/10.1016/B978-0-12-814062-8.00017-0.

50. Chatziparaskeva G, Papamichael I, Voukkali I *et al.* End-of-life of composite materials in the framework of the circular economy. *Microplastics* 2022;**1**:377–92.
51. Ballarin P, Dotelli G. Life cycle assessment of composite materials: a literature review. In: *Innovazione e Circolarit': il contributo del Life Cycle Thinking nel Green Deal per la neutralit' climatica*, 2022, pp. 476-82.
52. Dolganova I, Bach V, Rodl A *et al.* Assessment of critical resource use in aircraft manufacturing. *CircEconSust* 2022;**2**:1193–212.
53. Chatterjee B, Bhowmik S. Evolution of material selection in commercial aviation industry: a review. *Sustain Eng Prod Manuf Technol* 2019;199–219.
54. Mansor M, Nurfaizey A, Tamaldin N, Nordin M. Natural fiber polymer composites: utilization in aerospace engineering. In: *Biomass, Biopolymer-Based Materials, and Bioenergy*. Elsevier, 2019, 203-24.
55. Muhammad A, Rahman MR, Baini R, Bakri MK. Applications of sustainable polymer composites in automobile and aerospace industry. In: *Advances in Sustainable Polymer Composites*. Elsevier, 2021, 185-207.
56. Hagnell MK, Kumaraswamy S, Nyman T, Åkermo M. From aviation to automotive-a study on material selection and its implication on cost and weight efficient structural composite and sandwich designs. *Heliyon* 2020;**6**:e03716.
57. Nagaraju SB, Priya H, Girijappa YG, Puttegowda M. Lightweight and sustainable materials for aerospace applications. In: *Lightweight and Sustainable Composite Materials*. Woodhead Publishing, 2023, 157-78.
58. Jothibasu S, Mohanamurugan S, Vijay R *et al.* Investigation on the mechanical behavior of areca sheath fibers/jute fibers/glass fabrics reinforced hybrid composite for light weight applications. *J Ind Text* 2020;**49**:1036–60.
59. Vijay R, Singaravelu DL. Experimental investigation on the mechanical properties of cyperus pangorei fibers and jute fiber-based natural fiber composites. *Int J Polym Anal Charact* 2016; **21**:617–27.
60. Raghunathan V, Ayyappan V, Dhilip JD *et al.* Influence of alkali-treated and raw zanthoxylum acanthopodium fibers on the mechanical, water resistance, and morphological behavior of polymeric composites for lightweight applications. *Biomass Conv Bioref* 2023;1–13.
61. Julong D. Introduction to grey system theory. *J Grey Syst* 1989; **1**:1–24.
62. Singh M, Singh S. Multi-objective optimization of electro discharge machining of nimonic 75 using Taguchi-based gray relational analysis. *J Adv Manuf Syst* 2021;**20**:95–110.
63. Song H, Chen X, Zhang S, Xu L. Multi-objective optimization design of 6-UPS parallel mechanism based on Taguchi method and entropy-weighted gray relational analysis. *Appl Sci* 2022; **12**:5836.
64. Jam AS, Mosaffaie J, Tabatabaei MR. Raster-based landslide susceptibility mapping using compensatory MADM methods. *Environ Model Soft* 2023;**159**:105567.
65. Esangbedo MO, Abifarin JK. Cost and quality optimization taguchi design with grey relational analysis of halloysite nanotube hybrid composite: CNC machine manufacturing. *Materials* 2022; **15**:8154.
66. Sen PC, Hajra M, Ghosh M. Supervised classification algorithms in machine learning: a survey and review. In: *Emerging Technology in Modelling and Graphics: Proceedings of IEM Graph 2018*, 2020.
67. Parmezan AR, Souza VM, Batista GE. Evaluation of statistical and machine learning models for time series prediction: identifying the state-of-the-art and the best conditions for the use of each model. *Inform Sci* 2019;**484**:302–37.
68. T OT, Vartolomei MD, Rassweiler JJ *et al.* Artificial intelligence and machine learning in prostate cancer patient management'current trends and future perspectives. *Diagnostics* 2021; **11**:354.
69. Gehring C, Asai M, Chitnis R *et al.* Reinforcement learning for classical planning: viewing heuristics as dense reward generators. In: *Proceedings of the International Conference on Automated Planning and Scheduling*, Vol. 32 2022.
70. Goldberg DE. Genetic and evolutionary algorithms come of age. *Commun Acm* 1994;**37**:113–9.
71. Beasley D, Bull DR, Martin RR. An overview of genetic algorithms: part 1, fundamentals. *Univ Comp* 1993;**15**:56–69.
72. Karamnejadi AK, Kakouee A, Mollajafari M *et al.* Developed design of battle royale optimizer for the optimum identification of solid oxide fuel cell. *Sustainability* 2022;**14**:9882.
73. Park HS, Lee E, Choi SW *et al.* Genetic-algorithm-based minimum weight design of an outrigger system for high-rise buildings. *Eng Struct* 2016;**117**:496–505.
74. Gossling S, Lyle C. Transition policies for climatically sustainable aviation. *Trans Rev* 2021;**41**:643–58.
75. Buendia-Hernandez FA, Alvarez-Garcia FJ, OrtizBevia MJ, RuizdeElvira A. Dynamic modeling of air traffic emissions with a two variable system. *Int J Sustain Trans* 2021;**16**:1003–12.
76. Huang R, Riddle M, Graziano D *et al.* Energy and emissions saving potential of additive manufacturing: the case of lightweight aircraft components. *J Clean Prod* 2016;**135**:1559–70.
77. Al-Fatlawi A, Jormai K, Kovocs G. Optimal design of a fiber-reinforced plastic composite sandwich structure for the base plate of aircraft pallets in order to reduce weight. *Polymers* 2021; **13**:834.
78. Setlak L, Kowalik R, Lusiak T. Practical use of composite materials used in military aircraft. *Materials* 2021;**14**:4812.
79. Shrivastava S, Mohite P, Yadav T, Malagaudanavar A. Multi-objective multi-laminate design and optimization of a carbon fibre composite wing torsion box using evolutionary algorithm. *Compos Struct* 2018;**185**:132–47.
80. Seeger J, Wolf K. Multi-objective design of complex aircraft structures using evolutionary algorithms. *Proc Inst Mech Eng G-J Aer Eng* 2011;**225**:1153–64.
81. Morse L, Cartabia L, Mallardo V. Reliability-based bottom-up manufacturing cost optimisation for composite aircraft structures. *Struct Multidisc Optim* 2022;**65**:159.
82. Das M, Sahu S, Parhi D. Composite materials and their damage detection using ai techniques for aerospace application: a brief review. *Mater Today Proc* 2021;**44**:955–60.
83. Alhajahmad A, Mittelstedt C. Minimum weight design of curvilinearly grid-stiffened variable-stiffness composite fuselage panels considering buckling and manufacturing constraints. *Thin-Walled Struct* 2021;**161**:107526.
84. Nwambu C, Robert C, Alam P. Tensile behaviour of unaged and hygrothermally aged discontinuous bouligand structured CFRP composites. *Oxf Open Mater Sci* 2023;**3**:itac016.
85. Ricci JT, Coimbra RF, Gomes GF. Multiobjective optimization of the LASER aircraft wing's composite structural design. *Aeat* 2021;**93**:995–1010.
86. Ali JS, Haron SS. Stress analysis of composite aircraft wing using coupled fluid-structural analysis. *CFD Lett* 2021;**13**:78–86.

87. Sarangkum R, Wansasueb K, Panagant N *et al.* Automated design of aircraft fuselage stiffeners using multiobjective evolutionary optimisation. *IJVD* 2019;**80**:162–75.
88. Fan F, Zhu M, Fang K *et al.* Extraction and characterization of cellulose nanowhiskers from TEMPO oxidized sisal fibers. *Cellulose* 2022;**29**:213–22.
89. Samuel BO, Sumaila M, Dan-Asabe B. Multi-objective optimization and modeling of a natural fiber hybrid reinforced composite (PxGyEz) for wind turbine blade development using grey relational analysis and regression analysis. *Mech Adv Mater Struct* 2024;**31**:640–58.
90. Onyekwere O, Igboanugo A, Adeleke T. Optimisation of acetylation parameters for reduced moisture absorption of bamboo fibre using taguchi experimental design and genetic algorithm optimisation tools. *Nig J Tech* 2019;**38**:104–11.
91. Dharmalingam S, Meenakshisundaram O, Elumalai V, Boopathy RS. An investigation on the interfacial adhesion between amine functionalized luffa fiber and epoxy resin and its effect on thermal and mechanical properties of their composites. *J Nat Fib* 2021;**18**:2254–69.
92. Narayana VL, Rao LB. A brief review on the effect of alkali treatment on mechanical properties of various natural fiber reinforced polymer composites. *Mater Today Proc* 2021;**44**:1988–94.
93. Sabarinathan P, Annamalai V, Rajkumar K, Vishal K. Effects of recovered brown alumina filler loading on mechanical, hygrothermal and thermal properties of glass fiber'reinforced epoxy polymer composite. *Polym Polym Comp* 2021;**29**:S1092–S1102.
94. Valente M, Sambucci M, Sibai A, Iannone A. Novel cement-based sandwich composites engineered with ground waste tire rubber: design, production, and preliminary results. *Mater Today Sustain* 2022;**20**:100247.
95. Siva R, Kesavaram B, Martin JJ *et al.* Mechanical behavior of sisal and banana fiber reinforced hybrid epoxy composites. *Mater Today Proc* 2021;**44**:3692–6.

Oxford Open Materials Science, 2024, 4, 1–22
https://doi.org/10.1093/oxfmat/itae004
Research article